A novel stochastic linearization framework for seismic demand estimation of hysteretic MDOF systems subject to linear response spectra

Ioannis P. Mitseas[1*], Ioannis A. Kougioumtzoglou[2], Agathoklis Giaralis[3], Michael Beer[1,4,5]

[1]Institute for Risk and Reliability,

Faculty of Civil Engineering and Geodetic Science

Leibniz University Hannover,

Callinstr. 34, 30167, Hannover, Germany

e-mail: *mitseas@irz.uni-hannover.de, beer@irz.uni-hannover.de

[2]Department of Civil Engineering and Engineering Mechanics,

The Fu Foundation School of Engineering and Applied Sciences,

Columbia University,

500 West 120th Street, New York, NY 10027, USA.

e-mail: ikougioum@columbia.edu

[3]Department of Civil Engineering,

City, University of London,

Northampton Square, EC1V 0HB, London, UK

e-mail: agathoklis@city.ac.uk

[4]Institute for Risk and Uncertainty and School of Engineering,

University of Liverpool,

Peach Street, Liverpool L69 7ZF, UK

[5]School of Civil Engineering and Shanghai Institute of Disaster Prevention and Relief,

Tongji University,

No. 1239, Si Ping Rd. Shanghai 200092, China

Abstract

This paper proposes a novel computationally economical stochastic dynamics framework to estimate the peak inelastic response of yielding structures modelled as nonlinear multi degree-of-freedom (DOF) systems subject to a given linear response spectrum defined for different damping ratios. This is accomplished without undertaking nonlinear response history analyses (RHA) or, to this effect, constructing an ensemble of spectrally matched seismic accelerograms. The proposed approach relies on statistical linearization and enforces pertinent statistical conditions to decompose the inelastic d-DOF system into d linear single DOF oscillators with effective linear properties (ELPs): natural frequency and damping ratio. Each such oscillator is subject to a different stationary random process compatible with the excitation response spectrum with damping ratio equal to the oscillator effective critical damping ratio. This equality is achieved through a small number of iterations to a pre-specified tolerance, while peak inelastic response estimates for all DOFs of interest are obtained by utilization of the excitation response spectrum in conjunction with the ELPs. The applicability of the proposed framework is numerically illustrated using a 3-storey Bouc-Wen hysteretic frame structure exposed to the Eurocode 8 elastic response spectrum. Nonlinear RHA involving a large ensemble of non-stationary Eurocode 8 spectrum compatible accelerograms is conducted to assess the accuracy of the proposed approach in a Monte Carlo-based context. It is found that the novel feature of iterative matching between the excitation response spectrum damping ratio and the ELP damping ratio reduces drastically the error of the estimates (i.e., by an order of magnitude) obtained by non-iterative application of the framework.

1   INTRODUCTION

Practical design and assessment of structures for earthquake resistance commonly involves defining the seismic action through uniform hazard spectra (UHS) derived from probabilistic seismic hazard analysis based on ground motion prediction equations for spectral acceleration [1]. UHS provide the peak seismic response of linear viscously damped single-degree-of-freedom (SDOF) oscillators having a pre-specified probability to be exceeded in a given time period as a function of the natural period, T. They are developed for a nominal critical viscous damping ratio ζ_o, usually taken equal to 5%, and are complemented by damping adjustment factors [2] which reduce linear spectral ordinates in case a higher damping level from the nominal one needs to be adopted. Still, the vast majority of (ordinary) structures are expected to yield under the design seismic action since seismic codes and National regulatory agencies allow for structures to resist severe earthquakes through ductile behavior to achieve cost-effective design for reduced strength [3]. In this setting, the problem of estimating the peak *inelastic* response (i.e., seismic demand) for structures modelled as multi-degree-of-freedom (MDOF) systems subject to smooth *linear* response UHS arises naturally in code-compliant seismic structural design and assessment.

For any particular structure, this problem can be addressed through nonlinear response history analyses (RHA) applied to pertinent inelastic MDOF finite element (FE) models for a number of seismic ground motion records (GMs), whose average response spectrum matches

(i.e., is in close agreement with) the linear UHS within a certain range of natural periods centered at the fundamental structural natural period [4]. In this respect, putting the need for dependable inelastic FE modelling aside, code-compliant nonlinear RHA requires considering artificial UHS compatible accelerograms [5], and/or judicial GM selection from large databanks of recorded accelerograms which are further scaled/modified to match a given linear UHS [6]. Such steps necessitate specialized software, are subject to subjective preferences and experience, and are cumbersome for everyday seismic design (or assessment) of ordinary structures. Further, nonlinear RHA is computationally demanding itself, especially if a sufficiently large number of GMs are considered in the analysis to reduce the variability of peak inelastic response data observed [7] when only the minimum number of GMs allowed by current seismic codes (typically 7 pairs or less) is used [8].

In view of the above challenges, seismic codes and guidelines [9-12] favor the use of simplified methodologies for routine seismic design and assessment involving less demanding structural analysis steps compared to nonlinear RHA. In particular, the long-standing force-based seismic design methodology utilizes modal response spectrum-based analyses applied to linear MDOF FE models in conjunction with modal combination rules without requiring explicit structural seismic performance assessment [3]. Further, displacement-based seismic design and assessment methodologies supporting modern performance-based earthquake engineering utilize nonlinear static (pushover) analyses applied to MDOF FE models to derive detailed pushover curves. Structural capacity is then quantified through surrogate inelastic SDOF oscillators characterized by idealized backbone capacity curves fitted to the detailed pushover curves [13-16 and references therein]. In this context, design *seismic demand* is specified by *scaling the linear UHS ordinates* through modification factors derived by considering the peak seismic response of inelastic SDOF oscillators following idealized force-deformation hysteretic relationships, commonly following bilinear hardening backbone curves, to safeguard general applicability. Specifically, UHS ordinates are scaled by strength modification (or behavior) factors, R, in the traditional force-based design approach to derive constant-ductility inelastic spectra [17]. These spectra provide seismic design forces compatible with a pre-determined ductility μ (ratio of peak inelastic over yielding deformation) expected under the design seismic action. Initiated by the work of Veletsos and Newmark [18], R factors are specified through R-μ-T relationships (e.g., [19]) derived by application of nonlinear RHA to inelastic viscously damped SDOF oscillators with initial (pre-yield) natural period T and damping ratio ζ_o for large ensembles of judicially selected GMs [20]. Despite the availability of R-μ-T relationships for several different hysteretic force-deformation laws, codes of practice adopt R values pertaining to elastic perfectly-plastic SDOF oscillators known to yield conservative results for design purposes [21,22].

Moreover, in displacement-based seismic design and assessment UHS compatible inelastic seismic demand is obtained through scaling the UHS ordinates either by displacement modification factors [23], leading to constant-strength inelastic spectra, or by damping adjustment factors leading to heavily damped linear spectra [24,25]. Specifically, displacement modification factors are defined by the ratio of the peak response of an inelastic SDOF oscillator over the peak response of a linear SDOF oscillator under the same design seismic action, having common T (pre-yield for the inelastic) natural period and ζ_o damping ratio. These factors are determined either by "inverting" R-μ-T relationships or, directly, through application

of RHA for large ensembles of GMs [26] commonly considering bilinear hysteretic SDOF oscillators [27] consistent with capacity curves obtained from pushover analyses of MDOF systems [16]. On the other hand, damping adjustment factors for inelastic seismic demand estimation are derived through linearization techniques seeking to determine an equivalent linear SDOF system (ELS) with effective linear properties (ELPs), natural period $T_{ef}>T$, (or, equivalently, natural frequency $\omega_{ef}=2\pi/T_{ef}$), and damping ratio $\zeta_{ef}>\zeta_{o}$, such that its peak response under seismic excitation matches the peak response of an inelastic SDOF oscillator with pre-yield period T and damping ζ_{o} under the same excitation. Early linearization techniques assumed ductility-dependent secant stiffness at maximum displacement to define T_{ef} using the geometry of bilinear force-deformation loops reaching some ductility μ under harmonic excitation (e.g., [24,28]). Then, ductility-dependent ζ_{ef} is defined by enforcing equality criteria between the dissipated energy in the inelastic oscillator and in the ELS (e.g., [29 and references therein]). Nevertheless, secant stiffness-based linearization techniques were found to be deficient for displacement-based design and assessment (e.g., [14,30]). Therefore, numerous alternative linearization approaches yielding larger effective stiffness values from the secant stiffness have been developed for the task based on RHA of inelastic SDOF oscillators for large ensembles of recorded GMs (see e.g., [31,32,33 and references therein]). Some of these linearization approaches apply signal processing tools to the nonlinear response time-histories to define T_{ef} such as Fourier-based peak picking [34] and wavelet analysis [35], while others consider statistical fitting of heavily damped linear response spectra to inelastic spectra (e.g., [25,30,36-38]).

Recently, Giaralis and Spanos [39] established an alternative stochastic dynamics-based framework for code-compliant seismic demand estimation of bilinear hysteretic SDOF oscillators. The latter framework is considerably different from the previously reviewed approaches and does not require undertaking RHA. The steps of this framework, being of particular relevance to this paper, are delineated in Figure 1(a). They comprise: (I) the derivation of a stationary power spectrum representing a time-limited stationary stochastic process compatible in the median sense with a given linear response spectrum (i.e., a UHS) for ζ_{o} damping, (II) the application of *statistical linearization* to obtain ELPs (i.e., ω_{ef} and ζ_{ef}) from a viscously damped bilinear SDOF oscillator with pre-yield natural period T and damping ζ_{o} excited by the previously derived power spectrum, and (III) the use of these ELPs in conjunction with the given UHS and damping adjustment factors to estimate the peak inelastic response of the nonlinear oscillator (i.e., inelastic seismic demand for the UHS) through heavily damped spectra. Giaralis and Spanos [39] used the early stochastic averaging technique due to Caughey [40] to derive ω_{ef} and ζ_{ef} whose applicability is limited to relatively mild levels of nonlinear response (see also [41]). Later, Spanos and Giaralis [42] incorporated higher-order statistical linearization techniques in the above framework along with a system order reduction step allowing for treating a wide range of hysteretic force-deformation relationships (e.g., [43]), while enhancing the accuracy of seismic demand estimates compared to nonlinear RHA for UHS compatible GMs.
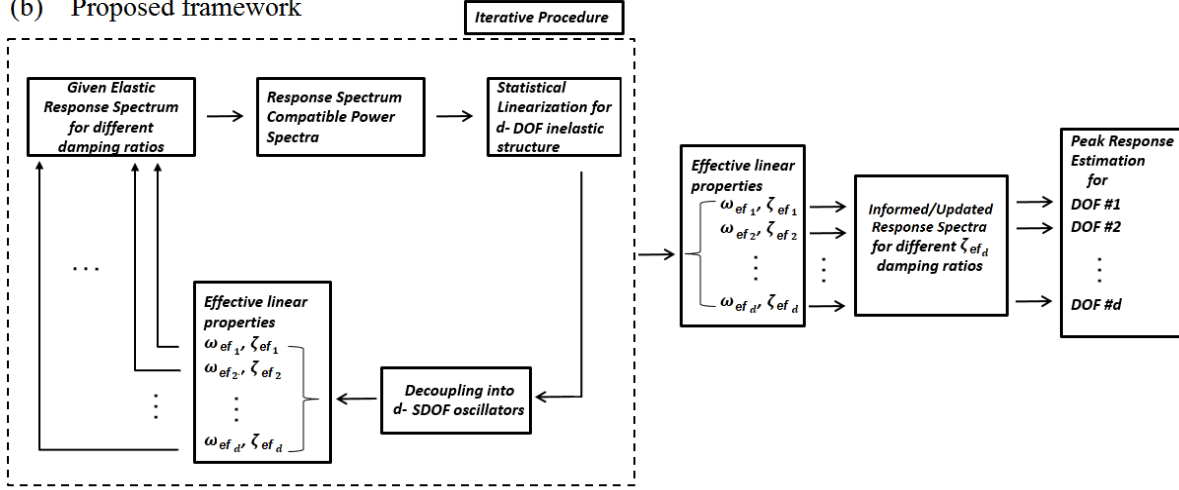
Figure 1. (a) Stochastic dynamics framework for SDOF inelastic oscillators (Giaralis and Spanos 2010), (b) Proposed stochastic dynamics framework for MDOF inelastic structures.

The above review reveals that current approaches for code-compliant inelastic seismic demand estimation consistent with a linear response spectrum (e.g., a UHS) are solely applicable to idealized inelastic (mostly bilinear) SDOF oscillators. Properties of these oscillators are obtained from capacity curves derived through static inelastic analyses to MDOF structural models which do not account for dynamic energy-dissipation phenomena (i.e., viscous and hysteretic damping) in the MDOF systems [33], while the static external forces do not reflect the properties of the UHS (e.g., frequency content). To this end, this paper proposes a novel stochastic dynamics-based seismic analysis framework for peak inelastic demand estimation directly applicable to MDOF systems exposed to a linear pseudo-acceleration response spectrum (e.g., UHS) without undertaking nonlinear RHA and, therefore, constructing ensembles of UHS compatible GMs, and without considering inelastic spectra developed for non-structure specific (generic) inelastic oscillators. The proposed framework seamlessly derives ELPs for each DOF of interest which depend explicitly on the nonlinear dynamic behavior of the MDOF system as captured through standard statistical linearization techniques for MDOF systems *and* on the shape and intensity of the input response spectrum; ultimately, it returns peak inelastic responses for each DOF individually using the derived ELPs in conjunction with heavily damped UHS defined by damping modification factors. This is achieved by relying on and significantly extending the approach of Giaralis and Spanos [39] in two distinct ways. Firstly, it replaces previously considered statistical linearization techniques appropriate only for SDOF oscillators in step (II) by the recently developed in Kougioumtzoglou and Spanos [44] approximate stochastic dynamics analysis method involving the *decoupling* of the nonlinear MDOF system with d DOFs into d number of ELSs characterized by d sets of ELPs, ω_{efj} and ζ_{efj} for $j=1,2,\ldots,d$, as shown pictorially in Figure 1(b). Secondly, it incorporates a novel iterative scheme to enforce equality, within some tolerance, between ζ_{efj} and the damping ratio of the input UHS. In this setting, it secures compliance with

the basic definition of the response/design spectrum which necessitates the considered linear/linearized oscillators and the imposed elastic response UHS to share the same damping premises. Clearly, the proposed approach treats in a rigorous and consistent manner, this well-detected critical point which has not received so far the appropriate attention in the literature. This is achieved by using different damping modification factors for each DOF j (see Figure 1(b)). The achieved consistency of the damping ratio of the input heavily damped spectrum with the damping ELPs enhances the accuracy of the inelastic seismic demand estimates as demonstrated in the numerical part of this work through pertinent nonlinear RHA in a Monte Carlo-based context.

It is noted in passing that the scope and steps involved of the herein developed framework are very different from the reliability-based tail statistical linearization approach proposed by Der Kiureghian and Fujimura [45]. The latter approach admits as input stochastic models consistent with magnitude-epicentral distance earthquake scenarios used to define the seismic action in beyond-codes-of-practice seismic design and assessment. On the other hand, the herein framework is tailored to facilitate code-compliant seismic demand estimation using linear UHS along with the well-established concept of damping modification factors to specify the seismic input action and aims to relax heuristic approximating assumptions made by current code-prescriptive simplified methods while being considerably less computationally demanding compared to nonlinear RHA for UHS compatible GMs.

In the remainder of this paper Section 2 reviews the mathematical background supporting the proposed framework, Section 3 presents an implementation algorithm of the framework and furnishes pertinent comments on its assumptions and practical usage, Section 4, presents a numerical application of the framework to a yielding building frame exposed to the Eurocode 8 UHS [11] and assesses its accuracy against nonlinear RHA data, and Section 5 summarizes main conclusions.

2   MATHEMATICAL BACKGROUND

This section reviews the mathematical details involved in undertaking the steps of (i) defining a power spectrum compatible in the median sense with a given seismic response spectrum, of (ii) applying the standard statistical linearization to a d-DOF inelastic structure to derive an equivalent linear d-DOF system, and of (iii) decoupling the previous equivalent linear system into d number of linear SDOF oscillators. Special attention is focused on discussing the various simplifications and assumptions made in support of numerical efficiency. The latter consideration is important in minimizing the computational cost/time of the framework in Figure 1(b) which requires the iterative application of the above three steps.

2.1 *Derivation of response spectrum compatible power spectra*

A computationally efficient numerical scheme is adopted to statistically fit a stationary Gaussian acceleration process $\ddot{\alpha}_g(t)$ of finite duration T_s, to a given/target linear pseudo-acceleration response spectrum, $S_a(\omega, \zeta)$ defined along the axis of natural frequencies ω for a fixed critical damping ratio ζ. The sought stochastic process is represented in the frequency domain by means of a non-parametric power spectrum computed on a uniform grid of frequencies using a recursive formula. This formula was originally derived by Cacciola et al.

[46], and utilized by Giaralis and Spanos [39,42] to obtain response spectrum compatible power spectra utilized in the statistical linearization-based approach summarized in Figure 1(a). It theoretically stems from the work of Vanmarcke [47] and relies on well-established concepts from the theory of linear random vibrations.

Specifically, consider the response displacement process $X_i(t)$ of a quiescent linear damped SDOF oscillator base excited by the process $\ddot{\alpha}_g(t)$. The nth order steady-state response spectral moment reads as (e.g., [48])

$$\lambda_{n,X_i} = \int_0^\infty \omega^n \frac{1}{(\omega_i^2 - \omega^2)^2 + (2\zeta_o \omega_i \omega)^2} G_{X_i}^{\zeta_o}(\omega) d\omega, \tag{1}$$

where ω_i and ζ_o are the natural frequency and the critical damping ratio of the SDOF oscillator, respectively, while $G_{X_i}^{\zeta_o}(\omega)$ is the one-sided power spectrum of the excitation process. Note that the above spectral moments do not account for the transient part of the response process. However, it has been numerically shown (e.g., [42]) that for SDOF oscillators with damping ratios $\zeta_o \geq 5\%$ and natural periods $T_i = 2\pi/\omega_i < 1.5s$, which are mostly pertinent in the analysis of ordinary low-to-mid-rise building structures, the response spectral moments determined via Eq.(1) are accurate as long as a sufficiently long duration of $T_s \geq 15s$ is assumed for the underlying stochastic process. Under this assumption, the time-limited power spectrum $G_{X_i}^{\zeta_o}(\omega)$ can be related to $S_a(\omega_i, \zeta_o)$ in a statistical manner via the concept of the "peak factor" η_{X_i} as in (e.g., [47])

$$S_a(\omega_i, \zeta_o) = \eta_{X_i} \omega_i^2 \sqrt{\lambda_{0,X_i}}. \tag{2}$$

In view of the above equation, the peak factor η_{X_i} can be interpreted as the scalar by which the steady-state standard deviation of the process $X_i(t)$ needs to be multiplied to estimate the threshold $S_a(\omega_i, \zeta_o)/\omega_i^2$ below which the peak deformation of the considered stochastically excited SDOF oscillator remains with some pre-specified probability p. The determination of the peak factor η_{X_i} requires knowledge of the first-passage probability, that is, the probability that the response process $X_i(t)$ crosses a predetermined threshold for the first time over a given time window. This has been a persistent mathematical problem in stochastic dynamics, but a number of sufficiently accurate for engineering purposes approximations exist. To this end, the peak factor can be estimated by the semi-empirical expression [47]

$$\eta_{X_i}(T_s, p) = \sqrt{2 \ln\{2 v_{X_i}[1 - \exp[-\delta_{X_i}^{1.2} \sqrt{\pi \ln(2 v_{X_i})}]]\}}, \tag{3}$$

where the mean zero crossing rate v_{X_i} and the spread factor δ_{X_i} of the stochastic response process $X_i(t)$ are defined as

$$v_{X_i} = \frac{T_s}{2\pi} \sqrt{\frac{\lambda_{2,X_i}}{\lambda_{0,X_i}}} (-\ln p)^{-1}, \tag{4}$$

and

$$\delta_{X_i} = \sqrt{1 - \frac{\lambda_{1,X_i}^2}{\lambda_{0,X_i} \lambda_{2,X_i}}}, \tag{5}$$

respectively. For the purposes of this work, it is reasonable to set the probability p in Eq.(4) equal to 0.5, such that $S_a(\omega_i, \zeta_o)$ in Eq.(2) is interpreted as the "median" pseudo-acceleration response spectrum. That is, half of the displacement response spectral ordinates of an ensemble of stationary samples of duration T_s compatible with the power spectrum $G_{X_i}^{\zeta_o}(\omega)$ lie below $S_a(\omega_i, \zeta_o)/\omega_i^2$ [39,47].

Note that the pseudo-acceleration response spectrum $S_a(\omega_i, \zeta_o)$ appearing in Eq.(2) can be estimated in a straightforward manner using Eqs. (1-5), given power spectrum $G_{X_i}^{\zeta_o}(\omega)$, duration T_s, and probability p. However, the derivation of a power spectrum $G_{X_i}^{\zeta_o}(\omega)$ compatible in the median sense (i.e., $p=0.5$) with a given response spectrum $S_a(\omega_i, \zeta_o)$ is appreciably more difficult and requires the solution of the "inverse" stochastic dynamics problem expressed by Eq.(2) (see e.g., [46,49-52]). Herein, the above aim is facilitated by adopting the following approximate formula for obtaining a reliable estimate of the variance of the response process $X_i(t)$ [47]

$$\lambda_{0,X_i} = \frac{G_{X_i}^{\zeta_o}(\omega_i)}{\omega_i^3} \left(\frac{\pi}{4\zeta_o} - 1 \right) + \frac{1}{\omega_i^4} \int_0^{\omega_i} G_{X_i}^{\zeta_o}(\omega) d\omega. \tag{6}$$

By substituting Eq.(6) to Eq.(2) and algebraically manipulating yields

$$S_a^2(\omega_i, \zeta_o) = \eta_{X_i}^2 \omega_i G_{X_i}^{\zeta_o}(\omega_i) \left(\frac{\pi - 4\zeta_o}{4\zeta_o} \right) + \eta_{X_i}^2 \int_0^{\omega_i} G_{X_i}^{\zeta_o}(\omega) d\omega. \tag{7}$$

Next, the integral in Eq.(7) is approximated by a sum over the uniform grid of M frequency points $\omega_i = \omega_b^l + (i - 0.5)\Delta\omega$; $i = 1,2,\dots M$ within the range (ω_b^l, ω_b^u). Finally, the following formula is reached by solving for the power spectrum evaluated at any frequency point ω_i [46]

$$G_{X_i}^{\zeta_o}(\omega_i) = \begin{cases} \frac{4\zeta_o}{\omega_i \pi - 4\zeta_o \omega_{i-1}} \left(\frac{S_a^2(\omega_i, \zeta_o)}{\eta_{X_i}^2} - \Delta\omega \sum_{q=1}^{i-1} G_{X_i}^{\zeta_o}(\omega_q) \right), & \omega_b^l < \omega_i < \omega_b^u \\ 0, & \omega_i \le \omega_b^l \end{cases}. \tag{8}$$

The above formula can be recursively applied for $i = 1,2,\dots M$ to evaluate the ordinates of the power spectrum $G_{X_i}^{\zeta_o}(\omega)$ at the M-1 frequency points ω_i lying $\Delta\omega$ apart in the range (ω_b^l, ω_b^u). In practice, the lower bound of this range, ω_b^l, is set equal to the lowest frequency for which Eq.(3) can be defined as discussed in [39]. Further, the upper bound, $\omega_b^u \ge \omega_M$, is the cut-off frequency above which $G_{X_i}^{\zeta_o}(\omega)$ attains negligible values. Lastly, it is important to note that the recursive application of Eq. (8) to obtain $G_{X_i}^{\zeta_o}(\omega_i)$ requires an estimate of the peak factor, $\eta_{X_i}^2$, for SDOF oscillators with ζ_o damping ratio and ω_i natural frequency. Reasonable estimates of this term are obtained through Eq. (3) in which the crossing rate ν_{X_i} and the spread factor δ_{X_i} are given by Eqs. (4) and (5), respectively, for an assumed excitation power spectrum, $N(\omega)$,

used as a proxy of $G_{X_i}^{\zeta_o}(\omega)$ in Eq. (1). Conveniently, both the crossing rate and the spread factor are independent of the amplitude of spectrum $N(\omega)$. Further, they are insensitive to the shape of $N(\omega)$ provided that it is sufficiently broad-band compared to the magnitude of the frequency response function (FRF) of the SDOF oscillators with ω_i and ζ_o properties (see e.g. [48]). In this respect, Cacciola et al. [48] and Giaralis and Spanos [39] derived power spectra $G_{X_i}^{\zeta_o}(\omega)$ achieving reasonably accurate levels of compatibility with $S_a(\omega, \zeta_o)$ by assuming analytically defined power spectral shapes $N(\omega)$ widely used to model the seismic strong ground motion in place of $G_{X_i}^{\zeta_o}(\omega)$ in Eq. (1). In this work, the filtered Kanai-Tajimi spectrum defined by [53]

$$N(\omega) = \frac{(\omega/\omega_f)^4}{\left(1 - (\omega/\omega_f)^2\right)^2 + 4\xi_f^2(\omega/\omega_f)^2} \frac{\omega_g^4 + 4\xi_g^2\omega_g^2\omega^2}{(\omega_g^2 - \omega^2)^2 + 4\xi_g^2\omega_g^2\omega^2}, \tag{9}$$

is used for the purpose where the parameters ω_g, ξ_g, ω_f, and ξ_f are constants that need to be judicially assumed. The Kanai-Tajimi parameters ω_g and ξ_g related to the soil "stiffness" and "damping" should be selected based on the ground conditions associated with the target response spectrum $S_a(\omega, \zeta_o)$ (see e.g., [5,54,55]). The parameters ω_f and ξ_f in Eq. (9) do not bear any physical significance: they govern the properties of a high-pass filter used to eliminate the spurious low frequency content allowed by the Kanai-Tajimi spectrum. These parameters can be arbitrarily set provided that ω_f, controlling the cut-off frequency of the high-pass filter, is reasonably low (typically, below π rad/s), while ξ_f, controlling the "steepness" of the filter in the frequency domain, is relative high (typically, above 0.80).

As a final remark, it is noted that the herein discussed approach is only one of the numerous proposed in the literature for the derivation of response spectrum compatible stationary power spectra in the median sense (see e.g., [49-51]). Regardless of the method used for this derivation, it is highlighted that the time-limited stationary power spectrum (and underlying stochastic process) is only used as a mathematical instrument to represent the seismic input action, defined in terms of a pseudo-acceleration response spectrum, in undertaking the statistical linearization step reviewed next. In this regard, the recursive application of Eq. (8) should be viewed only as a necessary "stepping stone" allowing for the application of the stochastic dynamics techniques discussed in the remainder of this section (see also Figure 1).

2.2 *Statistical Linearization for MDOF nonlinear structures under stationary seismic excitation*

Consider a nonlinear structural system with d number of DOFs base-excited by the Gaussian stationary acceleration stochastic process $\ddot{\alpha}_g(t)$, characterized in the frequency domain by the power spectrum $G_{X_i}^{\zeta_o}(\omega)$. The dynamic response of the structure is governed by the system of differential equations written in vector-matrix form as

$$\mathbf{M}\ddot{\mathbf{x}}(t) + \mathbf{C}\dot{\mathbf{x}}(t) + \mathbf{K}\mathbf{x}(t) + \mathbf{g}[\mathbf{x}(t), \dot{\mathbf{x}}(t)] = \mathbf{F}(t). \tag{10}$$

In Eq. (10) $\mathbf{x}(t)$, $\dot{\mathbf{x}}(t)$, and $\ddot{\mathbf{x}}(t)$ are the response displacement, velocity, and acceleration vectors relative to the base motion, respectively, normalized by a common nominal yielding displacement x_y. Further, $\mathbf{M}$, $\mathbf{C}$, and $\mathbf{K}$ denote the $(\mathrm{d} \times \mathrm{d})$ mass, damping, and stiffness

matrices, respectively, while $\mathbf{g}[\mathbf{x}(t), \dot{\mathbf{x}}(t)]$ is a nonlinear $(d \times 1)$ vector function of the variables $\mathbf{x}(t)$ and $\dot{\mathbf{x}}(t)$. Lastly, $\mathbf{F}(t) = -\mathbf{M}\gamma x_y^{-1} \ddot{\alpha}_g(t)$, is a $(d \times 1)$ zero mean, stationary random vector process where γ is the unit column vector. In this regard, $\mathbf{F}(t)$ can be expressed in the frequency domain by the spectral density matrix

$$S_{FF}(\omega) = \frac{G_{X_i}^{\zeta_o}(\omega)}{x_y^2} \mathbf{M}\gamma\gamma^T\mathbf{M}. \tag{11}$$

To this end, the standard spectral matrix solution procedure of the classical statistical linearization [41] is employed to estimate the response power spectral density matrix $\mathbf{S_{xx}}(\omega)$ of the nonlinear structure. This is achieved by considering a linearized version of Eq. (10) written as

$$\mathbf{M}\ddot{\mathbf{x}}(t) + (\mathbf{C} + \mathbf{C_{eq}})\dot{\mathbf{x}}(t) + (\mathbf{K} + \mathbf{K_{eq}})\mathbf{x}(t) = \mathbf{F}(t), \tag{12}$$

where the $(j, l)^{th}$ element of the equivalent linear matrices $\mathbf{C_{eq}}$ and $\mathbf{K_{eq}}$ are given by the expressions [56,57]

$$c_{j,l}^{eq} = E\left[\frac{\partial g_j}{\partial \dot{x}_l}\right], \tag{13}$$

and

$$k_{j,l}^{eq} = E\left[\frac{\partial g_j}{\partial x_l}\right], \tag{14}$$

in which $E[\cdot]$ is the mathematical expectation operator. The expressions in Eqs. (13) and (14) are derived by minimizing the difference (error) between the nonlinear system of equations in Eq. (10) and the linear system of equations in Eq. (12) in the mean square sense and by utilizing the standard assumption that the response process vector $\mathbf{x}(t)$ is Gaussian [41]. In this respect, the herein adopted statistical linearization approach approximates the response spectral density matrix of the nonlinear structure via the well-known frequency domain input-output relationship for linear systems [41]

$$\mathbf{S_{xx}}(\omega) = \mathbf{H_x}(i\omega)\mathbf{S_{FF}}(\omega)\mathbf{H_x}^*(i\omega), \tag{15}$$

where the superscript (*) denotes Hermitian transposition and the FRF matrix is defined as

$$\mathbf{H_x}(i\omega) = \left[\left[(\mathbf{K} + \mathbf{K_{eq}}) + \mathbf{M}(i\omega)^2\right] + i\omega(\mathbf{C} + \mathbf{C_{eq}})\right]^{-1}, \tag{16}$$

where i is the imaginary unit. Moreover, the Gaussian assumption for $\mathbf{x}(t)$ facilitates significantly the derivation of closed-form expressions for the integrals in Eqs. (13) and (14) for a variety of nonlinear functions $\mathbf{g}[\mathbf{x}(t), \dot{\mathbf{x}}(t)]$ used to model the inelastic response of seismically excited yielding structures (see e.g., [39,42]). For any such nonlinear/hysteretic model, the expressions in Eqs. (13) and (14) involve the response displacement and velocity covariance matrix terms determined by

$$E[x_j(t)x_l(t)] = \int_{-\infty}^{\infty} S_{x_j x_l}(\omega)\, d\omega \;\; and \;\; E[\dot{x}_j(t)\dot{x}_l(t)] = \int_{-\infty}^{\infty} \omega^2 S_{x_j x_l}(\omega)\, d\omega \tag{17}$$

where $S_{x_j x_l}(\omega)$ is the $(j, l)^{th}$ element of the response power spectrum matrix $\mathbf{S_{xx}}(\omega)$ in Eq. (15).

In this setting, the adopted statistical linearization scheme proceeds by solving the system of algebraic nonlinear equations in Eqs. (13-17). Any qualified nonlinear optimization algorithm may be employed for this task. Nevertheless, it is found that a simple iterative while-loop is sufficient to simultaneously satisfy Eqs. (13-17) until convergence of the elements of $\mathbf{C_{eq}}$ and $\mathbf{K_{eq}}$ matrices is achieved within a pre-specified tolerance [41]. These iterations are initialized by neglecting the $\mathbf{C_{eq}}$ and $\mathbf{K_{eq}}$ matrices in Eq. (16) in determining the covariance matrix terms in Eq. (17), which are then used to compute the elements of $\mathbf{C_{eq}}$ and $\mathbf{K_{eq}}$ via Eqs. (13) and (14).

The above statistical linearization step provides estimates of the normalized by x_y relative displacement and velocity auto-covariance terms for each $j=1,2,\ldots,d$ DOF of the nonlinear structure exposed to the response spectrum compatible power spectrum. These estimates are given as

$$E\left[x_j^2(t)\right] = \int_0^\infty \left(\left|H_{x_{j1}}(i\omega)\right|^2 m_1^2 + \left|H_{x_{j2}}(i\omega)\right|^2 m_2^2 + \cdots + \left|H_{x_{jd}}(i\omega)\right|^2 m_d^2\right) x_y^{-2}\, G_{X_i}^{\zeta_o}(\omega)d\omega, \quad (18)$$

and

$$E\left[\dot{x}_j^2(t)\right] = \int_0^\infty \omega^2 \left(\left|H_{x_{j1}}(i\omega)\right|^2 m_1^2 + \left|H_{x_{j2}}(i\omega)\right|^2 m_2^2 + \cdots + \left|H_{x_{jd}}(i\omega)\right|^2 m_d^2\right) x_y^{-2}\, G_{X_i}^{\zeta_o}(\omega)d\omega, (19)$$

respectively. Note that in Eqs.(18-19) the contributions of the off-diagonal terms (cross-terms) to calculating the mean square have been neglected, as their values are relatively negligible compared to the ones corresponding to the diagonal terms; see [53] and [59] for detailed discussions. From a computational implementation perspective, this is equivalent to considering a diagonal excitation power spectrum matrix in Eq.(11) of the form $\mathbf{S_{FF}}(\omega) = \frac{G_{X_i}^{\zeta_o}(\omega)}{x_y^2}\mathbf{M^2}$. The decoupling step reviewed in the next section utilizes the auto-covariances in Eqs. (18) and (19) to define linear SDOF oscillators with effective damping and natural frequency properties corresponding to each individual DOF.

2.3 Decoupling of the equivalent linear system and derivation of effective linear properties (ELPs)

Following the work of Kougioumtzoglou and Spanos [44], the equivalent linear system with d DOFs in Eq. (12) is next decomposed into d number of auxiliary SDOF linear oscillators each one assigned to a different DOF. It is assumed that all the auxiliary SDOF oscillators are base-excited by the same response spectrum compatible acceleration process, $\ddot{\alpha}_g(t)$, considered in deriving the equivalent linear system via statistical linearization. In this respect, for the jth DOF ($j=1,2,\ldots, d$), the equation of motion of the auxiliary SDOF oscillator reads as

$$\ddot{q}_j(t) + 2\zeta_{ef_j}\omega_{ef_j}\dot{q}_j(t) + \omega_{ef_j}^2 q_j(t) = -x_y^{-1}\ddot{\alpha}_g(t), \tag{20}$$

where $\ddot{q}_j(t)$, $\dot{q}_j(t)$, and $q_j(t)$ are the relative response acceleration, velocity, and displacement processes of the oscillator normalized by the yielding displacement x_y, and ω_{ef_j} and ζ_{ef_j} are the

effective natural frequency and damping ratio, respectively. These two effective linear properties (ELPs) characterizing each auxiliary SDOF oscillator are derived by the following two statistical conditions: the displacement and velocity response variances, $E[q_j^2(t)]$ and $E[\dot{q}_j^2(t)]$, respectively, of the auxiliary oscillator corresponding to the jth DOF are equal to the displacement and velocity response variances of jth DOF of the equivalent linear MDOF given by Eqs. (18) and (19), respectively. Mathematically, these conditions are written as

$$E[x_j^2(t)] = E[q_j^2(t)] = \int_0^\infty \left| H_{x_{\text{ef}_j}}(i\omega) \right|^2 x_y^{-2}\, G_{X_i}^{\zeta_o}(\omega) d\omega = \lambda_{0,q_j} x_y^{-2}, \quad (21)$$

and

$$E[\dot{x}_j^2(t)] = E[\dot{q}_j^2(t)] = \int_0^\infty \omega^2 \left| H_{x_{\text{ef}_j}}(i\omega) \right|^2 x_y^{-2}\, G_{X_i}^{\zeta_o}(\omega) d\omega = \lambda_{2,q_j} x_y^{-2}, \quad (22)$$

where

$$H_{x_{\text{ef}_j}}(i\omega) = \frac{1}{\left[(i\omega)^2 + i2\zeta_{\text{ef}_j}\omega_{\text{ef}_j}\omega + \omega_{\text{ef}_j}^2 \right]}. \quad (23)$$

To this end, Eqs. (21) and (22) in conjunction with Eqs. (18) and (19) constitute a nonlinear system of two algebraic equations which are solved for the two ELPs ω_{ef_j} and ζ_{ef_j} for each DOF. As in the case of the statistical linearization step, any nonlinear optimization algorithm can be used to find the ω_{ef_j} and ζ_{ef_j} that satisfy simultaneously the conditions in Eqs. (21) and (22). Alternatively, the two conditions may be satisfied through a standard iterative updating "while-loop" until convergence of the properties is achieved within some pre-specified tolerance.

Overall, for a d-DOF structure, a *d* number of 2x2 systems of nonlinear equations in Eqs. (21) and (22) need to be solved to derive *d* pairs of ELPs. In this manner, the MDOF equivalent linear system in Eq. (10) is decoupled into *d SDOF* linear oscillators. From a theoretical viewpoint, it is important to note that the above decoupling is very different from the one achieved by the well-known modal decomposition of linear structural dynamics which has been considered in conjunction with different statistical linearization schemes (e.g., [41,58]). In particular, note that the $q_j(t)$ response processes in Eq. (20) are not modal coordinates. Rather, they are direct estimates of the nonlinear normalized response displacement processes corresponding to each DOF of the nonlinear structure in Eq. (10) excited by a response spectrum compatible power spectrum.

From a practical viewpoint, it is highlighted that the obtained ELPs, ω_{ef_j} and ζ_{ef_j}, from the herein discussed decoupling step are amenable to a physical interpretation: they correspond to the stiffness and damping ratio of a linear SDOF oscillator, respectively. This is true for any kind of nonlinear vector function **g** in Eq. (10) and for any type of statistical linearization formulation adopted (note that higher-order statistical linearization schemes, as the one considered later in the illustrative example section, do not necessarily yield linearized systems in Eq. (12) corresponding to a physically plausible dynamical system- see also [42]). Moreover, numerical results reported in the literature demonstrate that the thus obtained ELPs are not mathematical artifacts. Rather, they appear to capture the inelastic response of any MDOF

system depending on the excitation intensity by taking on values in alignment with engineering intuition. For instance, stronger nonlinear response due to either a weaker structure and/or higher excitation intensity leads to heavier damped and/or more flexible auxiliary SDOF oscillators characterized by lower ω_{ef_j} and higher ζ_{ef_j} values [42,44,60]. In this regard, the effective natural frequency ω_{ef_j} has been considered in previous works to facilitate tracking and avoiding moving resonance phenomena [44,61,62], as well as to develop efficient approximate techniques for determining nonlinear system survival probability and first-passage probability density functions (e.g., [63,64]).

In this work, the above discussed attributes of the ELPs motivate their use to estimate the peak response of a given nonlinear MDOF structure exposed to a linear response spectrum $S_a(\omega_i, \zeta_o)$ as have been originally considered in [39] and [42] for the case of nonlinear SDOF systems. That is, by simply "reading" the linear spectral ordinates from the excitation response spectrum for all different ω_{ef_j} and ζ_{ef_j} corresponding to DOFs j=1,2,…,d (see also Figure 1). Conveniently, these spectral ordinates correspond to peak structural responses associated with each DOF and therefore no modal combination is required. The next section details the implementation of the framework in Figure 1(b) for response spectrum-based analysis of inelastic MDOF structures relying on the iterative application of the three steps discussed in this section.

3   IMPLEMENTATION OF PROPOSED FRAMEWORK

The three steps reviewed in the previous section are herein combined in a novel fashion to provide estimates of the peak inelastic response of nonlinear MDOF structures subject to a linear response spectrum $S_a(\omega, \zeta_o)$ without resorting to RHA. At the heart of the proposed approach lies the novel idea of iteratively updating the nominal damping ratio ζ_o of the input response spectrum by the effective damping properties, ζ_{ef_j}, obtained for each DOF until convergence. In this manner, input/output consistency of the damping ratio for each DOF is achieved. As will be evidenced in the next section in view of pertinent numerical results, this consistency provides improved accuracy of the peak inelastic response estimated for each DOF by $S_a(\omega_{\mathrm{ef}_j}, \zeta_{\mathrm{ef}_j})$ upon convergence of the proposed iterative procedure. In this section, the step-by-step implementation of the proposed stochastic dynamics framework in Figure 1(b) is presented with the aid of the flowchart in Figure 2, followed by a discussion on a number of important practical considerations in the application of the framework.

3.1 Mechanization of the framework

The proposed framework assumes as input an elastic response spectrum for a pre-specified damping ratio ζ_o as well as the equations of motion of the d-DOF nonlinear structure to be analyzed. It initializes by deriving a single response spectrum compatible power spectrum $G_{X_i}^{\zeta_o}(\omega)$ using Eq. (8) as shown in the upper three blocks of Figure 2. Standard statistical linearization is next applied *once* to the MDOF structure for this power spectrum using the formulation reviewed in section 2.2. In Figure 2, the global looping index value is k=0 for this first application of statistical linearization. A further local looping index, n, is also utilized in Figure 2 associated with the statistical linearization step which involves satisfying Eqs. (13-

17) using an iterative while-loop scheme. Convergence of the statistical linearization solution is assumed once the difference of all the elements of the $\mathbf{C_{eq}}$ and $\mathbf{K_{eq}}$ matrices lie below some small pre-specified thresholds β_1 and β_2, respectively. Next, the decoupling step detailed in section 2.3 is applied to derive d sets of ELPs ω_{ef_j} and ζ_{ef_j}, each one corresponding to a particular $j=1,2,\ldots,d$ DOF, taking as input the variances in Eqs. (18) and (19) derived from the statistical linearization step. Subsequently, a convergence check is made separately for each DOF to ensure that the difference between the damping ratio assumed in the definition of the input response spectrum and the derived effective damping ratio lies below a small pre-specified threshold β_3. In this first passage, the aforementioned check shown in Figure 2 as $\left|\zeta_{\text{ef}_j}^{(k)} - \zeta_{\text{ef}_j}^{(k-1)}\right| < \beta_3$ reads as $\left|\zeta_{\text{ef}_j}^{(1)} - \zeta_o\right| < \beta_3$ as a single response spectrum with the (given) damping ratio ζ_o applies. If the structure yields, this check will not be satisfied at this stage for any DOF. To this end, an updated response spectrum $S_a(\omega, \zeta_{\text{ef}_j}^{(1)})$ is defined, *different* for each DOF, and d different power spectra, $G_{X_i}^{\zeta_{\text{ef}_j}^{(1)}}(\omega)$, are computed using Eq. (8). Next, statistical linearization and decoupling steps are undertaken for all the different power spectra derived and a single check $\left|\zeta_{\text{ef}_j}^{(2)} - \zeta_{\text{ef}_j}^{(1)}\right| < \beta_3$ is made for each $G_{X_i}^{\zeta_{\text{ef}_j}^{(1)}}(\omega)$ corresponding to the particular j DOF. The damping ratio in defining the input response spectrum is updated for those DOFs that damping ratio convergence was not achieved and the procedure is repeated individually for these DOFs until convergence of $\zeta_{\text{ef}_j}^{(k)}$ with $\zeta_{\text{ef}_j}^{(k-1)}$ values, as shown in Figure 2. Clearly, the aforementioned procedure establishes a cyclic relationship between the, output, stochastically equivalent damping coefficients of the effective linear SDOF oscillators and the, input, damping ratios of the elastic response spectrum until input/output damping ratio consistency is achieved for all DOFs of interest. Lastly, once convergence between $\zeta_{\text{ef}_j}^{(k)}$ and $\zeta_{\text{ef}_j}^{(k-1)}$ is observed after k iterations for a j DOF, the peak inelastic response corresponding to this DOF can be readily estimated as a function of $S_a(\omega_{\text{ef}_j}^{(k)}, \zeta_{\text{ef}_j}^{(k)})$, that is by using the ordinate of the linear input response spectrum corresponding to the obtained ELPs from the proposed iterative algorithm.
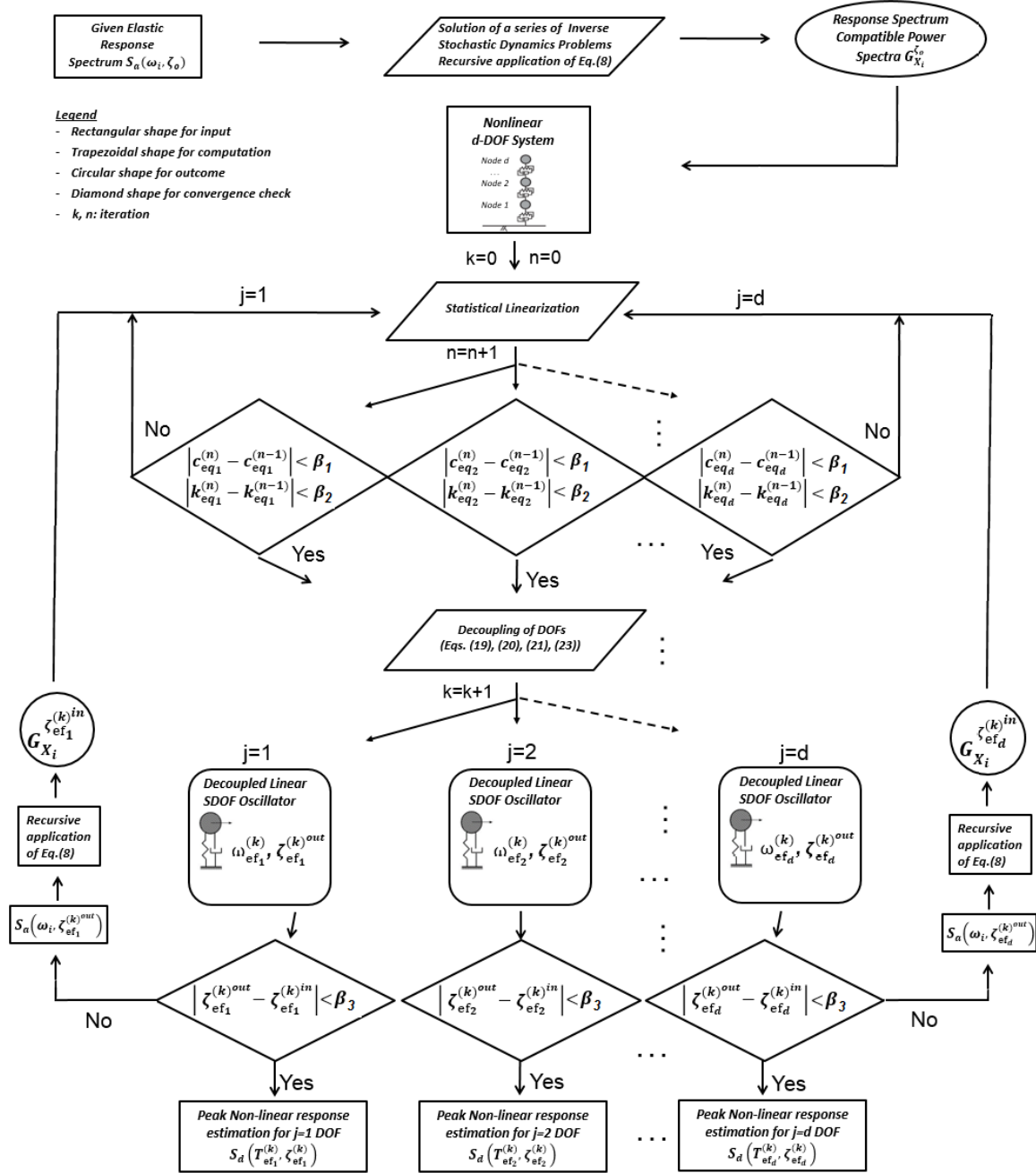
Figure 2. Implementation flowchart of the proposed framework.

3.2 Discussion

In view of the algorithmic implementation in Figure 2, comments on some important aspects and advantages of the proposed framework are herein discussed. Firstly, seismic excitation is conveniently represented by a linear (pseudo-acceleration) response spectrum, S_a, while the obtained peak inelastic response estimates are statistically consistent with this spectrum *in the mean sense*. This is achieved by setting the probability p equal to 0.5 in Eq. (4) such that S_a is treated as the median response spectrum in the derivation of power spectra using Eq. (8). The latter consideration serves well code-compliant seismic design and assessment of structures, as mentioned in the introduction, relying on mean seismic demands compatible with a specified mean linear UHS, S_a.

Secondly, the proposed framework assumes the availability of linear spectral ordinates for any damping ratio value $\zeta \geq \zeta_o$. This requirement stems from the fact that the effective damping ratios $\zeta_{\mathrm{ef}_j}^{(k)}$ will be higher from the nominal damping ratio ζ_o for yielding structures since statistical linearization accounts for the hysteretic energy dissipation through increased effective damping ratios [42]. To this end, the accuracy of the peak inelastic response estimates obtained by the proposed approach depends on the accuracy of the damping adjustment factors used to modify the UHS spectral ordinates for the nominal damping ratio ζ_o. Therefore, dependable damping adjustment factors need to be chosen which should be compatible with the seismotectonic environment for which the response spectrum S_a is associated with (see e.g., [2,65] and references therein). Conveniently, seismic design codes do include empirical formulae to define heavily damped spectra (see e.g., Eq. (A.2) in the Appendix) and, therefore, the proposed approach can be readily used in conjunction with code-defined UHS in practical applications.

Another important issue of practical concern is the fact that the SDOF oscillators in Figure 2 are associated directly with DOFs of the non-linear structure and not with modal responses of the underlying equivalent linear MDOF system. In this regard, the proposed approach does not involve any modal combination step: all response quantities lie in the physical space allowing for efficient peak response estimation directly from the response spectrum for each DOF. More importantly, the decoupling step can target only a small selected number of DOFs at will (e.g., it may be desired to obtain only the peak top floor lateral displacement in a multi-storey building) without incurring any additional approximation or loss of accuracy (i.e., as would be the case of a truncated modal combination without making use of all modes). This is because the contribution of all DOFs in the equivalent linear system is accounted for in computing the variances in Eqs. (18) and (19) in which all the *d* response cross-spectral density terms appear. Still, when the peak response for more than one DOFs is sought, the estimated peak responses will not happen at the same time and will not bear any particular sign. Therefore, it is not recommended to combine the peak response estimates *a posteriori* in an ad hoc fashion to evaluate peak structural responses of interest. For example, in the commonly encountered practical case that peak inter-storey drifts in seismically excited multi-storey buildings need to be computed, these should not be evaluated by subtracting peak floor displacements. Instead, the equations of motion need to be written directly in terms of the inter-storey drifts as exemplified in the illustrative application in the next section.

Lastly, pertinent remarks are due on the novel concept of iteratively updating the damping ratio of the input seismic spectrum based on the effective damping ratio individually for each DOF of interest. From a numerical viewpoint, convergence of this iterative procedure is the natural outcome of solving at the current iteration a "system identification" problem (i.e., the decoupling step discussed in section 2.3) to find ELPs for each DOF, in which both the given input/excitation (i.e., response spectrum compatible spectrum) and the pre-specified output/response (i.e., displacement and velocity variances obtained from statistical linearization step) are found by relying on the ELPs identified in the previous iteration. Indeed, the response spectrum compatible power spectrum for iteration index *k* is derived by solving the inverse problem in Eq. (2) in which the desired response is the median response spectrum with ELP damping identified in the *k*-1 iteration while the considered system is also a SDOF

with ELP damping from k-1 iteration. Further, the response variances in Eqs. (21) and (22) are found through linearization using the same power spectrum derived based on the ELP damping in k-1 iteration. Convergence, however, may not be monotonic in terms of peak response displacement as in most of the cases displacement spectral ordinates increase for oscillators with lower natural frequencies (longer periods), while statistical linearization to hysteretic structures of the softening kind yields equivalent linear oscillators with natural frequencies shifted towards lower frequencies reflecting on a reduced effective stiffness of yielding structures. Further comments on the rate and type of convergence of the herein proposed iterative procedure are included in the following section in view of pertinent numerical data. As a final remark, note that convergence of the above iterative procedure assigns response spectra of different damping ratios to each DOF which may be seen as counter-intuitive. Nevertheless, the variation of the damping ratios across different DOFs ensures that the value of ζ_{ef_j} found for each individual DOF is properly mapped onto a family of consistent input response spectral curves for different damping ratios and *vice versa*. Further, this variation is a consequence of the decoupling of the DOFs achieved by the adopted statistical criteria in Eqs. (21) and (22) and should be interpreted as a weighting factor applied consistently to the input earthquake excitation in a similar manner that participation factors scale differently the input seismic action for each mode in the standard modal response spectrum-based method of analysis for linear MDOF structures.

4   ILLUSTRATIVE APPLICATION

In this section the stochastic dynamics approach of Figure 2 is numerically illustrated by considering a yielding multi-storey frame structure subject to the Eurocode 8 elastic response spectrum [11] provided in the Appendix. Peak inelastic inter-storey drifts are derived by using ELPs in conjunction with the excitation response spectrum. The achieved accuracy of the predicted peak mean drifts is quantified by comparison with pertinent results derived from nonlinear RHA for an ensemble of time-histories compatible with the considered Eurocode 8 response spectrum. The presentation starts with a description of the adopted structure.

4.1 Inelastic frame structure

The three-story non-classically viscously-damped inelastic shear frame shown in Figure 3(a) is considered to exemplify the proposed approach. The lumped mass at the j-th floor, m_j, and the stiffness and damping coefficients of the j-th story, k_j and c_j, respectively, are reported in Figure 3(a) for j= 1,2,3. The inelastic behavior of the shear frame is governed by a hysteretic relationship between the resisting story shearing force and the inter-story drift. The same relationship is assumed for all three stories. Under these modelling assumptions, the resisting shearing force of the j-th story is given as the sum of an elastic and a hysteretic part as

$$\Phi_j(t) = \alpha k_j y_j(t) + (1 - \alpha) k_j z_j(t), \tag{24}$$

where α is the post-yield to pre-yield stiffness ratio, $y_j(t)$ is the inter-story drift normalized by the yielding displacement x_y, that is, $y_j(t) = (u_j - u_{j-1})/x_y$ where $u_j, j=0,1,2,3$ is the lateral floor displacement relative to the ground displacement with $u_0=0$ (Figure 3(a)), and $z_j(t)$ is a hysteretic state variable. In all the ensuing numerical work α is taken equal to 0.15 and the yielding displacement x_y is taken equal to 5cm.

Further, the parametric Bouc-Wen model [66] is adopted to govern the hysteretic storey shearing force versus normalized inter-storey drift relationship. This model has been used to capture the inelastic response of seismically excited frame structures (e.g., [67,68]), as the one herein considered, as well as of yielding structural components (e.g., [69]). This is due to its versatility to represent a wide range of hysteretic force-deformation experimental data from cyclic/seismic testing of structures and structural components (see e.g., [70]). The adopted model is herein introduced through the nonlinear differential equation

$$\dot{z}_j(t) = \left\{ A\dot{y}_j(t) - \beta\dot{y}_j(t)\big|z_j(t)\big|^n - \gamma\big|\dot{y}_j(t)\big|z_j(t)\big|z_j(t)\big|^{n-1} \right\}, \tag{25}$$

where parameters A, β, γ control the shape and the exponent n controls the smoothness of the hysteretic loops between the state variable z and, consequently, the shear force in Eq. (24) and the normalized inter-storey drift. In this work, the following values are adopted for the Bouc-Wen parameters $A = 1, \beta = \gamma = 0.5, n = 1$ to represent a smooth softening hysteretic behavior [66]. The backbone curve of the adopted Bouc-Wen model is plotted in Figure 3(b) (broken black curve) together with four hysteretic loops for different peak inter-storey drifts normalized to x_y obtained under harmonic excitation for steady-state conditions. It is seen that the model exhibits hysteresis even for drifts smaller than the nominal yielding deformation x_y (see [70] for a detailed discussion). Consequently, effective damping ratios with $\zeta_{ef_j} > \zeta_o$ are expected by application of statistical linearization even for excitations that will not deform the structure beyond the nominal x_y as discussed in [71] for the case of SDOF Bouc-Wen inelastic oscillators. Note that this is not the case of non-smooth idealized hysteretic models such as the bilinear model for which no hysteretic damping is exhibited unless $x>x_y$ [42]. For comparison, hysteretic loops of the non-smooth Bouc-Wen model computed by setting $n=15$ are plotted in Figure 3(b) (continuous grey curves).
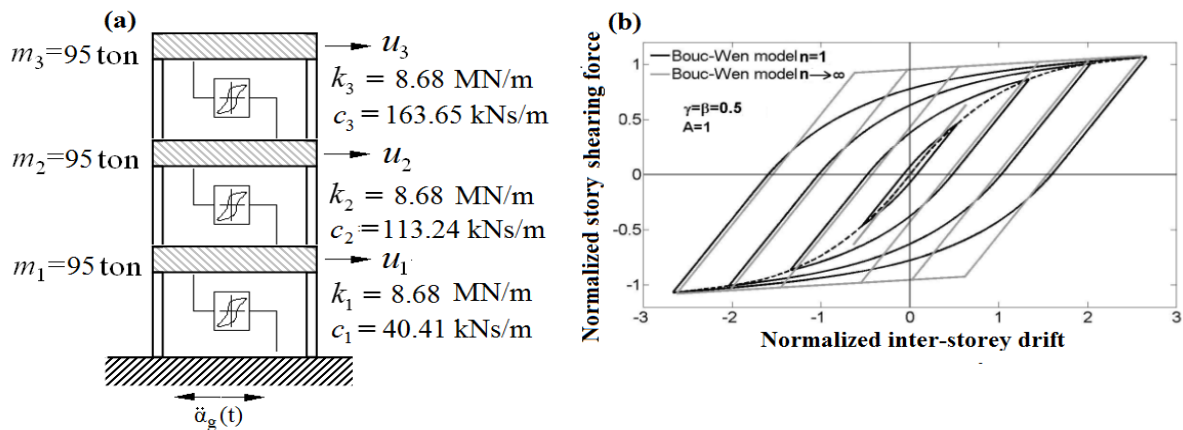

Figure 3. (a) Properties of the adopted inelastic three-storey shear frame; (b) Typical hysteretic loops of the adopted Bouc-Wen inelastic model.

4.2 Equations of motion for the non-linear and for the equivalent linear system

The equations of motion for the inelastic 3-storey frame in Figure 3(a) base excited by a stationary seismic acceleration process $\ddot{u}_g(t)$ can be written in the form of Eq. (10) by collecting in vector $\mathbf{x}$ the normalized by the yielding displacement inter-storey drifts and the hysteretic state variables for the three stories as

$$\mathbf{x}^{\mathbf{T}} = \{y_1\ y_2\ y_3\ z_1\ z_2\ z_3\}, \tag{26}$$

where the superscript "T" stands for matrix transposition. Then, the mass matrix in Eq. (10) is written as

$$\mathbf{M} = \begin{bmatrix} \mathbf{M_{11}} & \mathbf{0}_{3x3} \\ \mathbf{0}_{3x3} & \mathbf{0}_{3x3} \end{bmatrix}, \tag{27}$$

where

$$\mathbf{M_{11}} = \begin{bmatrix} m_1 & 0 & 0 \\ m_2 & m_2 & 0 \\ m_3 & m_3 & m_3 \end{bmatrix}, \tag{28}$$

and $\mathbf{0}_{3x3}$ is the 3-by-3 zero matrix, while the damping matrix is written as

$$\mathbf{C} = \begin{bmatrix} \mathbf{C_{11}} & \mathbf{0}_{3x3} \\ \mathbf{0}_{3x3} & \mathbf{I_{3x3}} \end{bmatrix}, \tag{29}$$

where

$$\mathbf{C_{11}} = \begin{bmatrix} c_1 & -c_2 & 0 \\ 0 & c_2 & -c_3 \\ 0 & 0 & c_3 \end{bmatrix}, \tag{30}$$

and $\mathbf{I}_{3x3}$ is the 3-by-3 identity matrix. Further, the stiffness matrix becomes

$$\mathbf{K} = \begin{bmatrix} \mathbf{K_{11}} & \mathbf{K_{12}} \\ \mathbf{0}_{3x3} & \mathbf{0}_{3x3} \end{bmatrix}, \tag{31}$$

where

$$\mathbf{K_{11}} = \begin{bmatrix} \alpha k_1 & -\alpha k_2 & 0 \\ 0 & \alpha k_2 & -\alpha k_3 \\ 0 & 0 & \alpha k_3 \end{bmatrix}, \tag{32}$$

and

$$\mathbf{K_{12}} = \begin{bmatrix} (1-\alpha)k_1 & -(1-\alpha)k_2 & 0 \\ 0 & (1-\alpha)k_2 & -(1-\alpha)k_3 \\ 0 & 0 & (1-\alpha)k_3 \end{bmatrix}. \tag{33}$$

Lastly, the vector $\mathbf{g}$ in Eq. (10) is written as

$$\mathbf{g}^{\mathbf{T}}[\mathbf{x}(t), \dot{\mathbf{x}}(t)] = \{0\ 0\ 0\ -g_1[\dot{y}_1(t), z_1(t)] - g_2[\dot{y}_2(t), z_2(t)]\ -g_3[\dot{y}_3(t), z_3(t)]\}. \tag{34}$$

where

$$g_j[\dot{y}_j(t), z_j(t)] = \dot{z}_j(t), \tag{35}$$

and the forcing vector reads as

$$\mathbf{F}(t)^{\mathbf{T}} = \{f_1(t)\ f_2(t)\ f_3(t)\ 0\ 0\ 0\}, \tag{36}$$

where $f_j(t) = -m_j \ddot{\alpha}_g(t)/x_y$.

Upon application of the standard statistical linearization, the equivalent linear matrices appearing in Eq. (12) take the form [41]

$$\mathbf{C_{eq}} = \begin{bmatrix} \mathbf{C_{eq11}} & \mathbf{C_{eq12}} \\ \mathbf{C_{eq21}} & \mathbf{C_{eq22}} \end{bmatrix}, \tag{37}$$

where

$$\mathbf{C_{eq11}} = \mathbf{C_{eq12}} = \mathbf{C_{eq22}} = \mathbf{0}_{3x3}, \tag{38}$$

and

$$\mathbf{C_{eq21}} = \begin{bmatrix} c_{eq1} & 0 & 0 \\ 0 & c_{eq2} & 0 \\ 0 & 0 & c_{eq3} \end{bmatrix}, \tag{39}$$

and

$$\mathbf{K_{eq}} = \begin{bmatrix} \mathbf{K_{eq11}} & \mathbf{K_{eq12}} \\ \mathbf{K_{eq21}} & \mathbf{K_{eq22}} \end{bmatrix}, \tag{40}$$

where

$$\mathbf{K_{eq11}} = \mathbf{K_{eq12}} = \mathbf{K_{eq21}} = \mathbf{0}_{3x3}, \tag{41}$$

and

$$\mathbf{K_{eq22}} = \begin{bmatrix} k_{eq1} & 0 & 0 \\ 0 & k_{eq2} & 0 \\ 0 & 0 & k_{eq3} \end{bmatrix}. \tag{42}$$

The elements c_{eq_j} and k_{eq_j} are given by the following closed-form expressions applicable for n=1 [43]

$$c_{eq_j} = \sqrt{\frac{2}{\pi}} \left[\gamma \frac{E(\dot{y}_j z_j)}{\sqrt{E(\dot{y}_j{}^2)}} + \beta \sqrt{E(z_j{}^2)} \right] - A, \tag{43}$$

and

$$k_{eq_j} = \sqrt{\frac{2}{\pi}} \left[\gamma \sqrt{E(\dot{y}_j{}^2)} + \beta \frac{E(\dot{y}_j z_j)}{\sqrt{E(z_j{}^2)}} \right], \tag{44}$$

respectively.

4.3 Derivation of Eurocode 8 compatible ELPs

The pseudo-acceleration elastic response spectrum prescribed by the current European seismic code, Eurocode 8, [11] for ground type B, nominal critical damping ratio $\zeta_o = 5\%$, and peak ground acceleration (PGA) equal to $0.36g$ is used to excite the structure in Figure

3(a). The adopted S_a spectrum is provided in the Appendix and plotted in Figure 4(a) (grey continuous curve) against the natural period $T=2\pi/\omega$.

Following the implementation of the proposed framework in Figure 2, a single S_a compatible power spectrum is first derived using Eq. (8) and is plotted in Figure 4(b). The duration T_s and the discetization step $\Delta\omega$ are taken equal to 20s and 0.1rad/s, respectively. The parameters assumed in Eq. (9) are $\xi_g = 0.78$, $\omega_g = 10.78\ rad\ s^{-1}$, $\xi_f = 0.90\ and\ \omega_f = 2.33\ rad\ s^{-1}$ which define a Clough-Penzien spectral shape plotted in Figure 4(c) compatible in the median sense with the herein adopted Eurocode 8 response spectrum derived in [55]. The spectral moments in Eq. (1) are computed using the default quadrature rule of the 'quad' built-in MATLAB function. The achieved level of compatibility between the power spectrum $G_{X_i}^{\zeta_o}(\omega)$ and the response spectrum S_a is assessed in Figure 4(a) by comparing the given S_a of Eurocode 8 with the response spectrum computed by Eq. (2) (broken line). A further assessment is made in terms of the criterion posed by Eq. (2) for $p=0.5$ as discussed in section 2.1 by undertaking a pertinent Monte Carlo based analysis. Specifically, an ensemble of 1000 stationary signals of 20s duration each compatible with the $G_{X_i}^{\zeta_o}(\omega)$ spectrum in Fig. 4(b) are generated using the spectral representation simulation method [71]. The median response spectrum of these signals are plotted (dotted line) in Figure 4(a). Satisfactory matching between the latter median response spectrum and S_a is observed which justifies the use of the ELPs derived as discussed below to approximate the peak inelastic inter-storey drifts of the structure in Figure 3(a) exposed to the response spectrum in Figure 4(a).
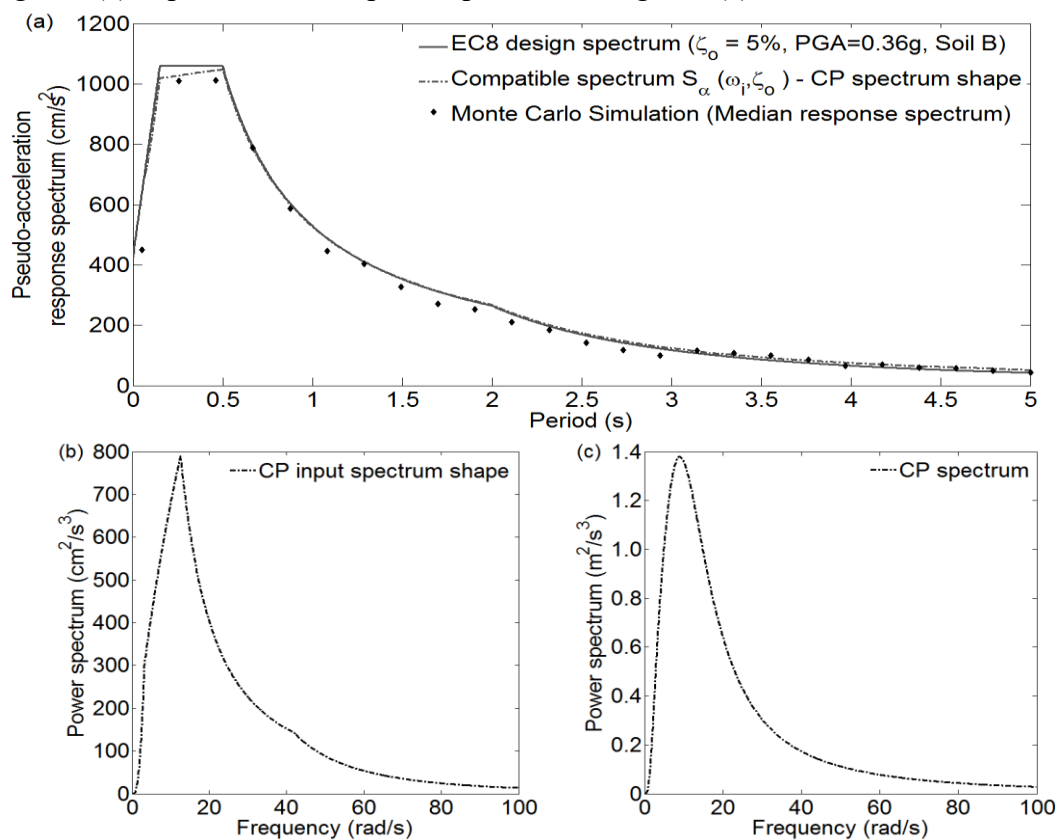

Figure 4. (a) Adopted Eurocode 8 response spectrum for 5% damping ratio and compatibility assessment with the power spectrum using Eq.(2) and NRHA. (b) Eurocode 8 response spectrum compatible power spectrum obtained by Eq.(8). (c) Clough Penzien spectral shape in Eq.(9) used to

Next, standard statistical linearization is applied for the derived power spectrum in Figure 4(b) using Eqs. (15)-(17) and (37)-(44). As discussed in sections 2.2 and 3.1, a simple iterative while-loop scheme is used to satisfy the previous expressions simultaneously, among possible alternatives (see e.g., [73]). The adopted thresholds for checking the convergence are set to $\beta_1=\beta_2= 10^{-4}$. Subsequently, a set of three $\omega_{\text{ef}_j}^{(1)}$ and $\zeta_{\text{ef}_j}^{(1)}$ ELPs $j=1,2,3$ corresponding to the three inter-storey drifts of the frame structure are derived by application of the decoupling step detailed in section 2.3. Then, three different power spectra compatible with the Eurocode 8 response spectrum given in the Appendix for critical damping ratios $\zeta_{\text{ef}_j}^{(1)}$ $j=1,2,3$ are derived using the same settings as those used to derive the initial $G_{X_i}^{\zeta_o}(\omega)$. Next, three different sets of ELPs for the previous three power spectra are obtained, one for each of the three DOFs and the process is iteratively repeated until the convergence check $\left|\zeta_{\text{ef}_j}^{(k)} - \zeta_{\text{ef}_j}^{(k-1)}\right| < \beta_3$ is satisfied for all $j=1,2,3$. For illustration purposes, a very small $\beta_3= 10^{-4}$ threshold has been adopted in the analysis.
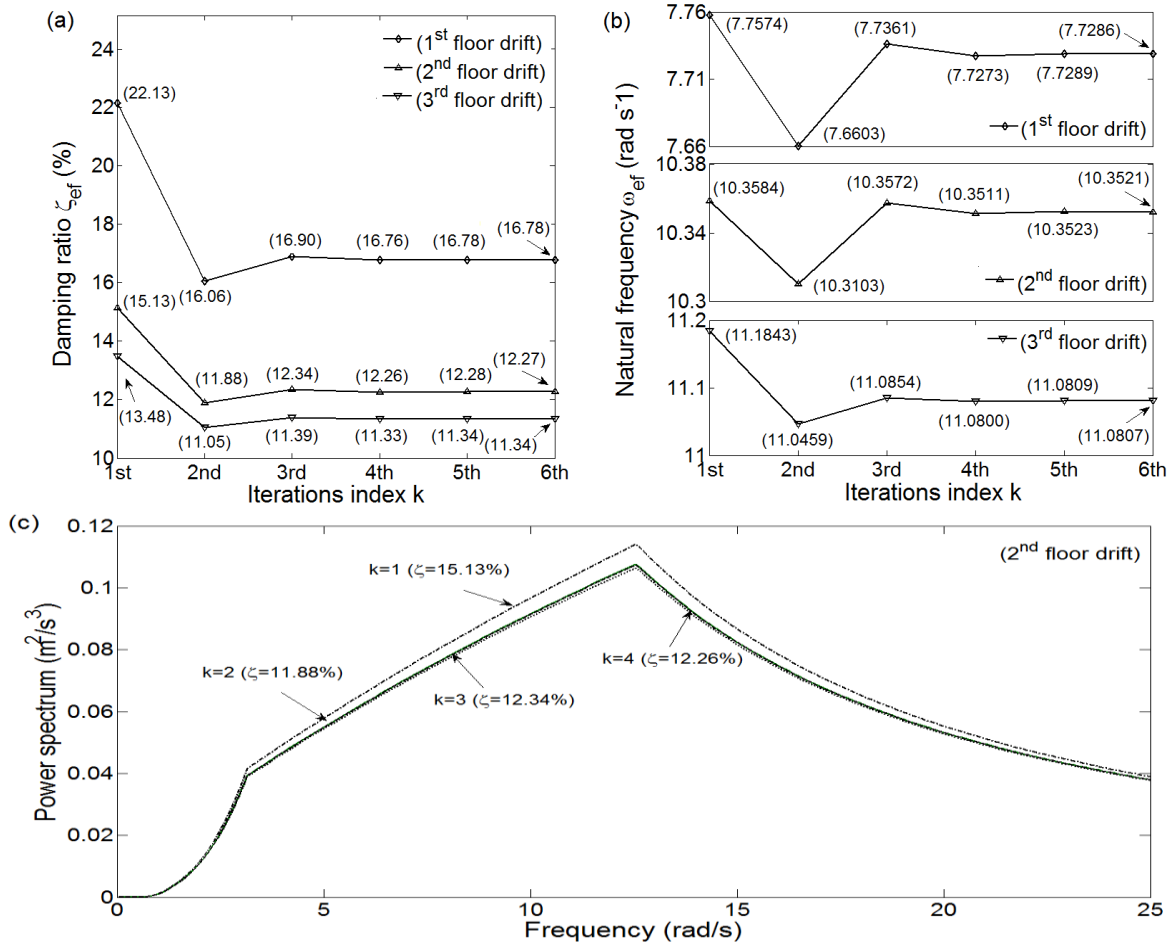

Figure 5. Effective natural frequency and damping ratio elements from successive iterations.

To illustrate the convergence achieved, the derived ELPs $\omega_{\text{ef}_j}^{(k)}$ and $\zeta_{\text{ef}_j}^{(k)}$ are plotted in Figures 5(a) and (b), respectively, for all three DOFs as a function of the iteration index k. Further, Figure 5(c) plots the input power spectra compatible with the Eurocode 8 response spectrum

iteratively updated based on the damping ELPs for the second DOF considered. It is seen that convergence is achieved after 3 iterations for all DOFs, but, as discussed in section 3.2, convergence is not monotonic. In particular, a single application of the statistical linearization and decoupling steps (k=1) overestimates ELPs for all DOFs. Upon updating the damping ratio of the response spectrum, different input power spectra for each DOF are derived yielding smaller ELP values (k=2), a further small adjustment towards higher values in the ELPs occurs in the subsequent iteration (k=3) and ELPs (as well as the input power spectra) remain practically unchanged for k>3 (convergence). It is noted that the effective natural frequency values do not fluctuate significantly; this is why they are not considered in checking for convergence. It is further important to note that the obtained ELPs are consistent with engineering intuition: softer and heavier damped effective SDOF oscillators are assigned to the floors (DOFs) that yield more (see Figure 7 for a verification based on NRHA), while effective damping ratios drop for input power spectra of reduced intensity reflecting on less energy dissipated through weaker nonlinear behavior. These observations confirm that the obtained ELPs by application of the proposed framework to inelastic MDOF structures bear physical significance as previously reported in [42] for the case of inelastic SDOF systems.

4.4 Peak inelastic response estimation using the ELPs and assessment via nonlinear RHA

Upon convergence of the effective damping ratios (i.e., $\left|\zeta_{ef_j}^{(k)} - \zeta_{ef_j}^{(k-1)}\right| < \beta_3$), the obtained pairs of ELPs are used to estimate the peak inter-storey drifts of the shearing frame in Figure 3(a) in conjunction with the input Eurocode 8 elastic response spectrum. This is pictorially shown in Figure 6 where the Eurocode 8 spectrum is plotted against the natural period for the three different values of damping ratio $\zeta_{ef_j}^{(6)}$, $j=1,2,3$ found, in terms of spectral acceleration, S_α, left vertical axis, and in terms of spectral displacement, S_α/ω^2, right vertical axis. The three peak inelastic inter-storey drifts are read on the right vertical axis using the ($T_{ef_j} = 2\pi/\omega_{ef_j}^{(6)}$, $\zeta_{ef_j}^{(6)}$) pairs indicated on the figure. All estimated drifts are above the considered yielding drift of 5cm which indicates that the structure enters well into the inelastic range (see also Figure 3(b) and discussion on the assumed smooth Bouc-Wen model). It is seen that drifts decrease with height, which is expected from a shear-type frame with uniformly distributed mass in elevation, even though higher effective damping ratios, ζ_{ef_j}, are found for the effective SDOF oscillators assigned to the lower floors. Evidently, this is associated with ω_{ef_j} taking on lower values, or equivalently T_{ef_j} becoming longer at lower floors leading to increase displacement demands despite the increase of the damping ratio. Overall, these observations confirm that the ELPs derived from the proposed method lead to reasonable peak drift response estimates.
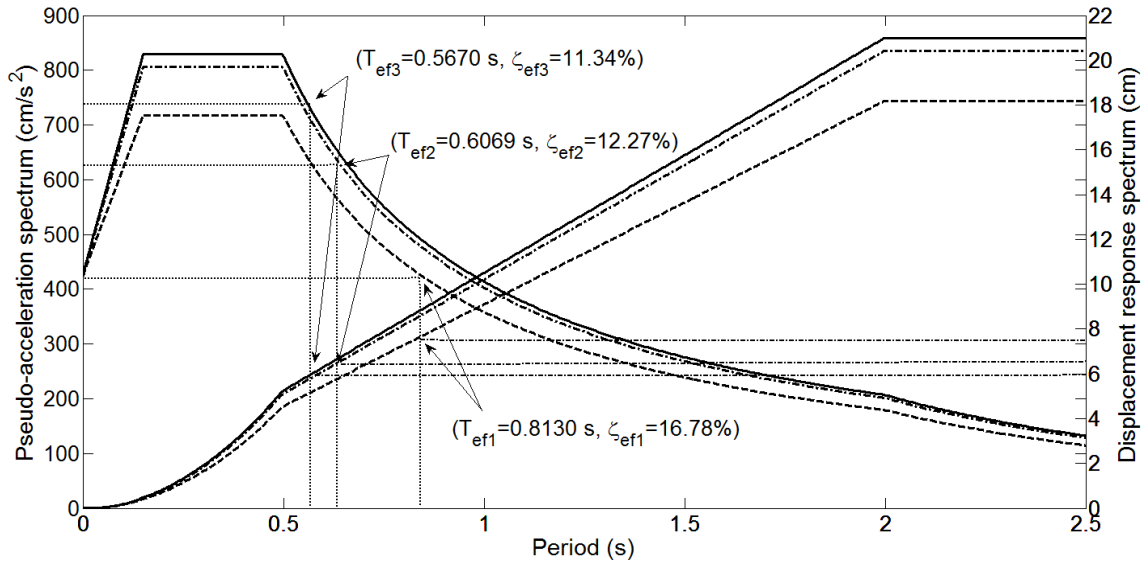
Figure 6. Peak inter-storey drifts estimation using the ELPs for k=6 in Figure 5 in conjunction with the Eurocode 8 response spectrum of the Appendix for different damping ratios.

To further assess the accuracy of the above derived peak response estimates, nonlinear RHA for an ensemble of 5000 artificial acceleration time-histories compatible in the mean sense with the Eurocode 8 elastic response spectrum for 5% damping is conducted. Specifically, the considered time-histories are non-stationary in amplitude: an arbitrarily chosen time-history out of the ensemble is plotted in Figure 7(a). Their average and median response spectra achieve a good level of matching with the Eurocode 8 spectrum as shown in Figure 7(b). These time-histories are derived by first generating 5000 stationary realizations compatible with the Clough-Penzien spectrum in Figure 4(c) using the spectral representation method [72]. Next, these realizations are multiplied by an envelope function in time derived in [55] to achieve average spectral matching with the herein considered Eurocode 8 spectrum. Lastly, the nonlinear differential equations of motion in Eq. (10) are numerically integrated for the above ensemble via a standard fourth order Runge-Kutta algorithm, for $\mathbf{x}$, $\mathbf{M}$, $\mathbf{C}$, $\mathbf{K}$, $\mathbf{g}$, and $\mathbf{F}$ defined in Eqs. (26)-(36).
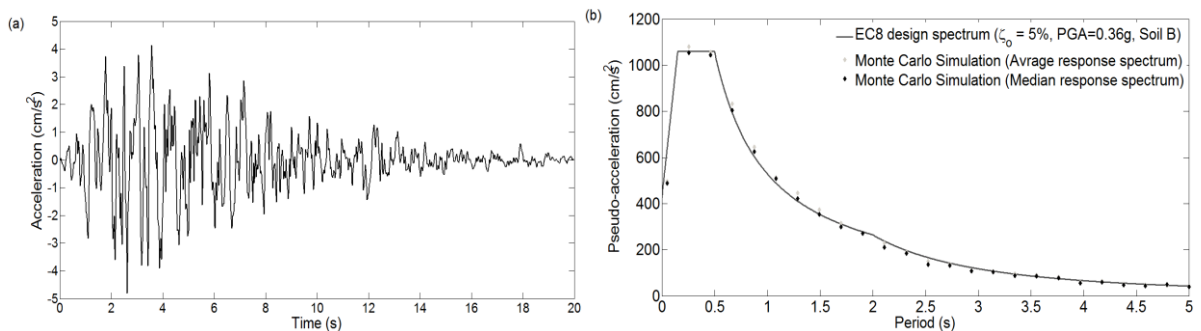

Figure 7. (a) Time-history of an arbitrarily chosen artificial accelerogram from an ensemble of 5000 compatible with the Eurocode 8 spectrum with 5% damping. (b) Average and median response spectra of an ensemble of 5000 artificial accelerograms vis-à-vis the Eurocode 8 spectrum with 5% damping.
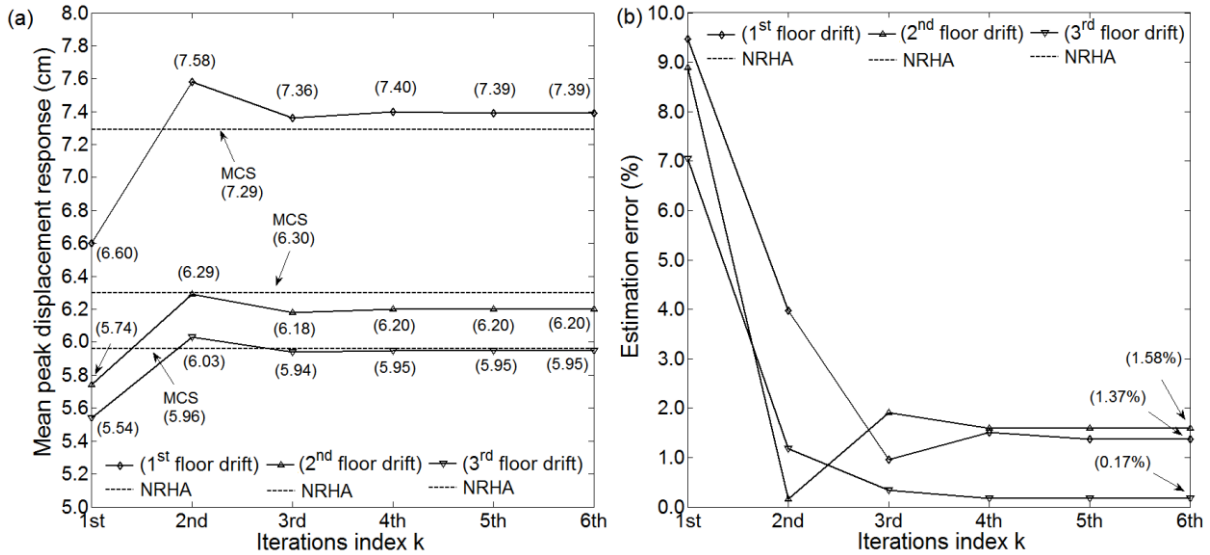
Figure 8. Comparison of peak inter-storey drift estimates obtained from the proposed method for different iterations with ensemble average peak inter-storey drifts from NRHA. (a) Absolute values, (b) Percentage difference (error).

Figure 8(a) compares the *ensemble average* of the peak response inter-storey drifts obtained from NRHA within a Monte Carlo simulation context (treated as "accurate" values hereafter), with the inter-storey drifts estimated using the ELPs reported in Figures 5(a) and 5(b) in conjunction with the excitation Eurocode 8 response spectrum as illustrated in Figure 6. Further, Figure 8(b) reports the percentage error between the inter-storey drifts from nonlinear RHA with those obtained by the proposed method for all 6 iterations performed. It is seen that enhanced accuracy compared to nonlinear RHA results is achieved for the DOFs (stories) exhibiting milder nonlinear behavior. The latter can be gauged through the average ductility demand obtained from nonlinear RHA results as 7.29/5= 1.46, 6.30/5= 1.26, and 5.96/5= 1.19 for the 1st, 2nd, and 3rd story, respectively. This observation is in perfect alignment with pertinent numerical results reported in [42] for bilinear hysteretic SDOF oscillators and in [71] for Bouc-Wen SDOF oscillators for a wide range of ductility demands using ELPs derived by the same statistical criteria in Eqs. (21) and (22) for peak inelastic response estimation. The fact that accuracy deteriorates with stronger nonlinearity is readily attributed to the well-studied in the literature level of accuracy with which statistical linearization approximates inelastic response statistics in Eqs. (18) and (19) (see e.g. [41] and references therein).

Nevertheless, the most important observation in Figure 8 is the remarkable improvement of accuracy achieved through the iterative updating of the excitation response spectrum based on the equivalent damping ratio for each DOF. In particular, the accuracy improves by about one order of magnitude upon convergence (i.e., for k>=3), compared to the results obtained by a non-iterative application the framework (i.e., a single passing through the three steps reviewed in section 2). Even more important is the fact that this improvement does not depend on the level of nonlinearity exhibited. For example, the same reduction by 84% to the estimation error for both the 1st and 2nd story drifts between no response spectrum updating (k=1) and 5 times response spectrum updating (k=6) is noted, even though the 1st floor exhibits 16% higher ductility demand from the 2nd floor. In this respect, it can be argued that the novel concept of updating the damping ratio of the excitation response spectrum iteratively for each DOF individually to achieve consistency with the effective damping ratio benefit substantially

the accuracy of the proposed stochastic dynamics framework in comparison with pertinent Monte-Carlo simulation-based results derived by nonlinear RHA.

5 CONCLUDING REMARKS

A computationally efficient nonlinear stochastic dynamics based framework has been proposed for estimating the peak inelastic response of hysteretic MDOF structural systems subject to a given family of linear response UHS defined for various damping ratios through modification factors, without the need to undertake nonlinear RHA. The proposed framework initiates by the derivation of a power spectrum representing a time-limited stationary process compatible with the given response spectrum for a nominal damping ratio treated as the median spectrum. Next, estimates of second-order response statistics for a considered inelastic MDOF structure are obtained through standard statistical linearization for the derived power spectrum. Then, for each DOF of interest of the MDOF structure, an effective linear SDOF oscillator is defined such that it has the same response displacement and velocity variance with those of the MDOF structure estimated by the statistical linearization step. The above three steps are repeated iteratively for each monitored DOF upon updating the damping ratio of the excitation response spectrum with the effective damping ratio of each linear SDOF whose value reflects on the level of the nonlinearity exhibited by the MDOF structure. Upon convergence of the damping ratio of the response spectrum with the effective damping ratio for each DOF (i.e., equality within some small error), the properties of each effective SDOF oscillator (ELPs) are used together with the excitation response spectrum for different damping ratios to obtain peak response estimates for the MDOF structure.

It has been argued, based on heuristic nonlinear structural dynamics arguments, that convergence of the above novel iterative procedure lying at the core of the proposed framework will be observed for typical yielding seismically excited structures. This has been demonstrated in view of numerical results involving a three-storey shear frame excited by a Eurocode 8 UHS whose nonlinear behavior is modelled by the Bouc-Wen model. Moreover, nonlinear RHA involving an ensemble of 5000 non-stationary accelerograms whose mean response spectrum matches closely the considered Eurocode 8 UHS has been conducted to study the accuracy of the proposed framework. It has been found that the accuracy deteriorates for higher levels of nonlinearity gauged via average peak seismic inter-storey ductility demands for each floor of the frame considered which is consistent with the approximations involved in the statistical linearization step. However, it has been shown that considerably improved accuracy is achieved by the proposed framework through the iterative damping ratio updating procedure, independently of the exhibited level of nonlinearity. The latter observation qualifies the herein proposed approach as a rather advantageous analysis tool for preliminary/cursory seismic design and assessment of yielding structures based on seismic demands posed by a given response spectrum representing the seismic hazard.

Still, it is recognized that the accuracy of the proposed framework as stronger non-linear behavior is exhibited is inevitably constraint by the well-reported in the literature accuracy of statistical linearization and, therefore, it may not provide sufficiently accurate peak response estimates for low-performing structures. Nevertheless, it is envisioned that the considered approach can significantly facilitate code-compliant design and assessment of relatively mildly

yielding MDOF structures following any hysteretic force-displacement law treatable by means of statistical linearization. Comparisons of the proposed framework with existing simplified approaches for seismic demands estimation warrants further research left for future work.

APPENDIX: ADOPTED EUROCODE 8 ELASTIC RESPONSE SPECTRUM

The Eurocode 8 elastic pseudo-acceleration response spectrum for peak ground acceleration 0.36g (g=981 cm/s^2) and ground type B used in the numerical work of this paper is defined by [11]

$$S_\alpha(T,\zeta) = 0.432\text{g} \times \begin{cases} 1 + \dfrac{T}{0.15}(2.5\delta - 1), & 0 \le T \le 0.15 \\ 2.5\delta, & 0.15 \le T \le 0.5 \\ \dfrac{1.25\delta}{T}, & 0.50 \le T \le 2 \\ \dfrac{2.5\delta}{T^2}, & 2 \le T \le 4 \end{cases} \qquad (A.1)$$

where

$$\delta = \sqrt{\frac{10}{5+\zeta}} \ge 0.55, \qquad (A.2)$$

T=2π/ω is the natural period and *ζ* is the critical damping ratio as a percentage.

REFERENCES

[1] McGuire RK. *Seismic Hazard and Risk Analysis. Monograph MNO-10*, Oakland: Earthquake Engineering Research Institute; 1995.

[2] Lin YY, Miranda E, Chang KC. Evaluation of damping reduction factors for estimating elastic response of structures with high damping. *Earthquake Engineering and Structural Dynamics 2005;34(11):1427-1443*.

[3] Avramidis I, Athanatopoulou A, Morfidis K, Sextos A, Giaralis A. *Eurocode-compliant seismic analysis and design of r/c buildings: concepts, commentary and worked examples with flowcharts.* Geotechnical, Geological and Earthquake Engineering, Springer, New York. doi:10.1007/978-3-319-25270-4, 2016.

[4] Katsanos EI, Sextos AG, Manolis GD. Selection of earthquake ground motion records: a state-of-the-art review from a structural engineering perspective. *Soil Dynamics and Earthquake Engineering 2010*; 30(4):157–169.

[5] Giaralis A, Spanos PD. Wavelet-based response spectrum compatible synthesis of accelerograms-Eurocode application (EC8), *Soil Dynamics and Earthquake Engineering 2009*, 29, pp. 219–235.

[6] Katsanos EI, Sextos AG. ISSARS: an integrated software environment for structure-specific earthquake ground motion selection. *Advances in Engineering Software 2013; 58:70–85.*

[7] Araujo M, Macedo L, Marques M and Castro JM. Code-based record selection methods for seismic performance assessment of buildings. *Earthquake Engineering and Structural dynamics 2015, 45(1): 129-148.*

[8] Beyer K, Bommer JJ. Selection and scaling of real accelerograms for bi-directional loadings: a review of current practice and code provisions. *Journal of Earthquake Engineering 2007; 11:13–45.*

[9] Federal Emergency Management Agency FEMA, *Prestandard and commentary for the seismic rehabilitation of buildings.* Rep. No. FEMA-356, Washington, D.C., 2000.

[10] BSSC, *NEHRP recommended provisions for seismic regulations for new buildings and other structures.* Building Seismic Safety Council for the Federal Emergency Management Agency (FEMA Rep. 368, 369), Washington, DC, 2003.

[11] CEN. Eurocode 8: *Design of Structures for Earthquake Resistance - Part 1: General Rules, Seismic Actions and Rules for Buildings. EN 1998-1: 2003 E.* Comité Européen de Normalisation, Brussels, 2004.

[12] Federal Emergency Management Agency FEMA. *Improvement of nonlinear static seismic analysis procedures.* Rep. No. FEMA-440, Washington, DC, USA; 2005.

[13] Fajfar P. A nonlinear analysis method for performance-based seismic design, *Earthquake Spectra 2000; 16(3): 573-592.*

[14] Chopra AK and Goel RK. Evaluation of NSP to estimate seismic deformation: SDF systems. *Journal of Structural Engineering, ASCE 2000; 126: 482-490.*

[15] Priestley MJN, Calvi GM and Kowalsky MJ. *Displacement-based seismic design of structures*, IUSS Press, Pavia, 2007.

[16] De Luca F, Vamvatsikos D and Iervolino I. Near-optimal piecewise linear fits of static pushover capacity curves for equivalent SDOF analysis, *Earthquake Engineering and Structural Dynamics 2013,* 42: 523-543.

[17] Newmark NM, Hall WJ. Earthquake spectra and design. *Berkeley: Earthquake Engineering Research Institute,* 1982.

[18] Veletsos AS and Newmark NM. Effect of inelastic behavior on the response of simple systems to earthquake motions. *Proceedings of the 2nd World Conference on Earthquake Engineering, 2,* pp. 895–912. Japan, 1960.

[19] Miranda E, Bertero VV. Evaluation of strength reduction factors for earthquake-resistance design. *Earthquake spectra 1994,* 10:357-79.

[20] Karakostas CZ, Athanasios CJ, Kappos AJ and Lekidis VA. Site-dependent design spectra and strength modification factors, based on records from Greece. *Soil Dynamics and Earthquake Enginering 2007*, 27:1012-1027.

[21] Chopra AK. *Dynamics of structures. Theory and applications to earthquake engineering.* 2nd ed. Prectice-Hall; 2001.

[22] Kappos AJ. Evaluation of behaviour factors on the basis of ductility and overstrength studies. *Eng Struct 1999;21(9):823–35.*

[23] Miranda, E. Inelastic displacement ratios for structures on firm sites, *J. Struct. Eng. 2000, 126(10), 1150–1159.*

[24] Gulkan, P. and Sozen, M. Inelastic response of reinforced concrete structures to earthquake motion, *ACI Journal 1974, 71, 604–610.*

[25] Iwan WD. Estimating inelastic response spectra from elastic spectra. *Earthquake Eng Struct Dyn. 1980; 8:375–88.*

[26] Miranda, E. Estimation of inelastic deformation demands of SDOF systems. *J. Struct. Eng. 2001; 127(9), 1005–1012.*

[27] Chopra AK, Chintanapakdee C. Inelastic deformation ratios for design and evaluation of structures: single-degree-of-freedom bilinear systems. *J Struct Eng ASCE 2004; 130:1309–19.*

[28] Rosenblueth E., and Herrera I. On a Kind of Hysteretic Damping, *ASCE Journal of Engineering Mechanics 1964;* 90(4), 37–48.

[29] C.A. Blandon, M.J.N. Priestley Equivalent viscous damping equations for direct displacement based design, *J Earthquake Eng. 2005; 9 (2) pp. 257-278.*

[30] Guyader AC, Iwan WD. Determining equivalent linear parameters for use in a capacity spectrum method of analysis. *Journal of Structural Engineering 2006;132:59–67.*

[31] Miranda E, Ruiz-Garcia J. Evaluation of approximate methods to estimate maximum

inelastic displacement demands. *Earthquake Engineering and Structural Dynamics* 2002; 31:539–560.

[32] Lin YY, Miranda E. Evaluation of equivalent linear methods for estimating targeted displacements of existing structures. *Eng Struct 2009; 31:3080–3089.*

[33] Monteiro R, Marques M, Adhikari G, Casarotti C, Pihno R. Spectral reduction factors evaluation for seismic assessment of frame buildings, *Engineering structures 2014, 77, 129-142.*

[34] Levy R, Rutenberg A, Qadi Kh. Equivalent linearization applied to earthquake excitations and the *R –μ–T o* relationships. *Eng Struct 2006; 28:216–28.*

[35] Makris N and Kampas G. Estimating the "effective period" of bilinear systems with linearization methods, wavelet and time-domain analyses: from inelastic displacements to modal identification. *Soil Dynamics and Earthquake Engineering 2013;* 45, 80-88.

[36] Iwan WD, Gates NC. The effective period and damping of a class of hysteretic structures. *Earthquake Eng Struct Dyn. 1979; 7:199–211.*

[37] Kwan WP, Billington SL. Influence of hysteretic behavior on equivalent period and damping of structural systems. *J Struct Eng ASCE 2003;129:576–85.*

[38] Liu T, Zordan T, Zhang Q, Briseghella B. Equivalent viscous damping of bilinear hysteretic oscillators, *Journal of Structural Engineering, ASCE 2015; 141(11) 10.1061/(ASCE)ST.1943-541X.000126*

[39] Giaralis, A., Spanos, P.D. Effective linear damping and stiffness coefficients of nonlinear systems for design spectrum based analysis. *Soil Dynamics and Earthquake Engineering 2010*, 30(9): 798-810.

[40] Caughey TK. Random excitation of a system with bilinear hysteresis. *J Appl Mech ASME 1960; 27:649–52.*

[41] Roberts J. B., Spanos P.D. *Random vibration and statistical linearization*, New York: Dover Publications, *2003.*

[42] Spanos P.D. and Giaralis A. Third-order statistical linearization-based approach to derive equivalent linear properties of bilinear hysteretic systems for seismic response spectrum analysis. *Structural Safety 2013, 44, 59-69.*

[43] Wen, Y.K. Equivalent linearization for hysteretic systems under random excitation, *J.*

Applied Mech., ASME 1980; 47, pp. 150-154.

[44] Kougioumtzoglou I. A., Spanos P.D. Nonlinear MDOF system stochastic response determination via a dimension reduction approach, *Computers and Structures 2013; 126: 135-148.*

[45] Der Kiureghian A and Fujimura K. Nonlinear stochastic dynamic analysis for performance-based earthquake engineering, *Earthquake Eng Struct Dyn 2009; 38:719–738.*

[46] Cacciola P, Colajanni P, Muscolino G. Combination of modal responses consistent with seismic input representation. *J Struct Eng ASCE 2004; 130: 47–55.*

[47] Vanmarcke EH. Structural response to earthquakes. *Seismic risk and engineering decisions, C. Lominitz and E. Rosenblueth, eds. Elsevier, New York, 287-337, 1976.*

[48] Vanmarcke EH. Properties of spectral moments with applications to random vibration. *J Eng Mech 1972; 98(2), 425-446.*

[49] Kaul MK. Stochastic characterization of earthquakes through their response spectrum. *Earthquake Eng Struct Dyn 1978; 6:497–509.*

[50] Pfaffinger DD. Calculation of power spectra from response spectra. *J Eng Mech ASCE 1983; 109:357–72.*

[51] Park YJ. New conversion method from response spectrum to PSD functions. *Journal of Engineering Mechanics, ASCE 1995;* 121: 1391-1392.

[52] Falsone G. and Neri F. Stochastic modelling of earthquake excitation following the EC8: power spectrum and filtering equations, *European Earthquake Engineering 2000; 14 (1), 3-12.*

[53] Clough RW and Penzien J. *Dynamics of Structures. Second Edition.* Mc-Graw Hill, New York, 1993.

[54] Lai SP. Statistical characterization of strong ground motions using power spectral density function. *Bulletin of the Seismological Society of America 1982;* 72: 259-274.

[55] Giaralis, A., Spanos, P. D. Derivation of response spectrum compatible non-stationary stochastic processes relying on Monte-Carlo peak factor estimation. *Earthquake Structures 2012, 3, 581-609.*

[56] Kazakov IE. Generalization of the method of statistical linearization to multidimensional

systems. *Automation and Remote Control 1965; 26: 458-464.*

[57] Atalik TS and Utku S. Stochastic linearization of multi-degree-of-freedom non-linear systems. *Earthquake Engineering and Structural Dynamics 1976;* 4: 411-420.

[58] Fang T and Wang Z.N. A Generalization of Caughey's Normal Mode Approach to Nonlinear Random Vibration Problems, *AIAA Journal 1986, Vol. 24, No. 3, pp. 531-534.*

[59] Lutes L. D., Sarkani S., 2004. Random vibrations: analysis of structural and mechanical systems, Elsevier.

[60] Giaralis, A., Kougioumtzoglou, I.A. and Dos Santos, K. Non-stationary stochastic dynamics response analysis of bilinear oscillators to pulse-like ground motions. In: 16th World Conference on Earthquake Engineering 2017 - 16WCEE (January 9-13, 2017, Santiago, Chile), paper #3401, pp.12.

[61] Tubaldi E., Kougioumtzoglou I. A., Nonstationary stochastic response of structural systems equipped with nonlinear viscous dampers under seismic excitation, *Earthquake Engng Struct. Dyn 2014;, DOI: 10.1002/eqe.2462.*

[62] Mitseas, I.P., Kougioumtzoglou, I.A., Beer, M. An approximate stochastic dynamics approach for nonlinear structural system performance-based multi-objective optimum design. *Structural Safety 2016*; vol. 60, p. *67-76.*

[63] Spanos P.D., Kougioumtzoglou I.A., Survival probability determination of nonlinear oscillators subject to evolutionary stochastic excitation, *ASME J Appl. Mech. 2014; 81(5),051016 1–9.*

[64] Mitseas, I.P., Kougioumtzoglou, I.A., Spanos P.D., Beer, M. Nonlinear MDOF system Survival Probability Determination Subject to Evolutionary Stochastic Excitation. *Strojniški vestnik - Journal of Mechanical Engineering 2016; 62 7-8, 440-451.*

[65] Hubbard DT and Mavroeidis GP. Damping coefficients for near-fault ground motion response spectra. *Soil Dyn Earthquake Eng 2011; 31:401–17.*

[66] Wen, Y.K. Method for random vibration of hysteretic systems, *Journal of the Engineering Mechanics Division ASCE 1976; 102, pp. 249-263.*

[67] Wen YK., Eliopoulos D., Method for nonstationary random vibration of inelastic structures, *Probabilistic Engineering Mechanics 1994; 9: 1–2, 115-123.*

[68] Guo AX, Xu YL, Wu B. Seismic reliability analysis of hysteretic structure with

viscoelastic dampers, *Engineering structures 2002; 24, pp. 373-383.*

[69] Karavasilis, T.L., Kerawala, S., Hale, E. Hysteretic model for steel energy dissipation devices and evaluation of a minimal-damage seismic design approach for steel buildings. *J. Constr. Steel Res. 2012, 70, 358-554 367.*

[70] Ikhouane, F., Rodellar, J., Hurtado, J.E. Analytical characterization of hysteresis loops described by the Bouc–Wen model. *Mech. Adv. Mater. Struct. 2006; 13, 463–472.*

[71] Giaralis A. and Spanos PD. Derivation of equivalent linear properties of Bouc-Wen hysteretic systems for seismic response spectrum analysis via statistical linearization. *In: Proceedings of the 10th HSTAM International Congress on Mechanics (May 25-27, 2013, Chania, Greece) (eds: Beskos D and Stavroulakis GE), Technical University of Crete Press.*

[72] Shinozuka M., Deodatis G., Simulation of stochastic processes by spectral representation, *Applied Mechanics Reviews 1991, vol. 44, no. 4, pp. 191-204.*

[73] Silva, F.L., Ruiz, S.E. Calibration of the equivalent linearization Gaussian approach applied to simple hysteretic systems subjected to narrow band seismic motions, *Structural Safety 2000; 22, pp. 211-231.*